WILEY

Moving towards high-energy rechargeable Mg batteries- Status and challenges

Kiran Kumar Reddy Reddygunta[a], *Behara Dilip Kuma* [b*]

[a]Smart Materials Research and Device Technology (SMaRDT) Group, Department of Pure and Applied Chemistry, University of Strathclyde, Glasgow, UK
[b]Department of Chemical Engineering, JNTUA College of Engineering, Anantapur, AP, INDIA
*Corresponding Author: dileepbh.chemengg@jntua.ac.in

Abstract

Lithium-ion batteries (LIBs) have gained significant market share in the field of consumer electronics, grid storage and hybrid electric vehicles, because of their exceptional energy densities per unit volume (area or weight) compared to other electrochemical energy storage systems. But they do approach their maximum practical capacities and the efforts are underway to explore future battery systems with enhanced energy density than LIBs. There has been growing interest in incorporating multivalent ions such as Zn^{2+}, Mg^{2+} and Al^{3+}, since they offer greater volumetric energy densities than their monovalent counterparts like LIBs and Sodium-ion batteries. It has long been acknowledged that replacing Lithium with Magnesium (Mg) ions in the battery systems has many potential benefits such as low cost, excellent rate capability and high energy density, ease of handling and eco-friendly. Yet, little breakthrough has been made in the advancement of rechargeable magnesium batteries (RMBs) since its first discovery in 2000. The success of RMBs has been hindered by the slow electrode kinetics and also the formation of passive layers on Mg metal surfaces seriously effecting its performance during Mg^{2+} ion magnesiation/de-magnesiation. This chapter provides comprehensive knowledge on the background of rechargeable Mg battery, principles and cell configuration, discussing key advancements made in the last two decades in terms of their electrode materials and electrolytes. Finally, a brief note on future research strategies are outlined.

Keywords: rechargeable magnesium batteries; Energy storage; electrodes; electrolyte; intercalation/de-intercalation

1. Background

A clear understanding of the electrode-electrolyte interphases is required to realize the application of Mg-ion batteries.

The human need for energy is growing at an enormous pace leading to the depletion of fossil fuels and also effecting the environment. Hence the demand for cleaner, greener and sustainable (solar, tidal and wind) energy resources have been the topic of interest of interest among the research community and praised as an alternative to the conventional fossil fuels. Nevertheless, these sustainable energy resources are intermittent owing to weather, geographic conditions and may not serve the commercial applications continuously, compelling the need for advanced energy storage devices (ESDs).[1-3]

ESDs such as lithium-ion battery (LIB) and lead acid battery technology has enjoyed a great success in powering consumer electronics and smart grids benefiting from their electrochemical features such as high energy densities, lower discharge rates, enormous throughput and eco-friendliness.[4, 5] Although, LIBs are driving the current energy market, they are plagued by limited lithium (Li) metal reserves, dendrite formation, high cost and safety issues limiting its growth. Hence, scientists are investigating diverse earth abundant metals including sodium (Na), zinc (Zn), aluminum (Al), calcium (Ca) and magnesium (Mg) that has the potential to replace Li metal without compromising their performance and safety issues. Al, Zn and Mg are widely employed as anodes in rechargeable batteries and have similar working mechanisms like Li metal. Their unique features such as smaller ionic radius, multi-electron reactions and comparably lower oxidation potentials allows them to deliver high energy capacity and specific capacity.[6, 7] There is no denying that Al, Zn and Mg cannot serve as competitive as LIBs, considerable efforts are being made to improve their charge storage performance and requires time to challenge LIBs or even surpass them.

Table 1 summarizes some of the important features of Mg compared to Li, Na, Ca, Al and Zn for battery applications. Among the earth abundant metals, Magnesium batteries (Mg) is termed as an ideal alternative to LIBs, because Mg metal possess lower redox potential (an advantage for high volumetric energy throughput), high coulombic efficiency. Moreover, Mg metal is free from dendrite formation (in certain electrolytes) making it safer, lasts longer unlike LIBs which are constrained to dendrite formation.[8, 9] According to the reports, Mg is eighth most abundant alkaline earth metal paving way for less expensive electrode materials than Li metal.[10] Also, manufacturing RMBs does not release any toxic compounds making them safer and cleaner way to store electrochemical energy at lower cost. Furthermore, the electrochemical deposition and dissolution of Mg is a two-electron process, resulting in a high volumetric capacity of 3832 mA h cm^{-3}, making it potentially beneficial if a smaller battery packaging is required. Despite their intriguing characteristics stated above, divalent Mg^{2+} ions suffer from sluggish electrode kinetics due to their strong polarizing nature which often leads to little or even zero capacity hampering their commercial applications.[11] Hence substantial research is in progress to develop finest material combinations for high performing RMBs. The goal of this chapter is to discuss the advancements made in cathode, anode and electrolyte technology towards Mg electrochemistry. Lastly, challenges involved and research perspectives in their development are discussed.

2. Cell configuration and working mechanism

A typical RMB is not different with respect to corresponding lithium or sodium ion counterparts when it comes to cell configuration or working mechanism. As illustrated in Figure 1, the active components of RMBs are:

- Anode made of pure metal or other sources rich in Mg.
- Electrolyte acting as ionic conducting medium transport Mg^{2+} ions easily from the anode to cathode and vice versa. Higher ionic conductivity materials are generally used as the electrolyte so that Mg ions traverse back and forth easily.

- Separator – A microporous film placed between the anode and cathode to avoid short circuit and self-discharge. Separator acts as a ion selective membrane which allows only ions to pass through them but not electrons.
- Cathode [Q] which involves in redox reaction with Mg and thus generating electrons. RMBs performance is greatly influenced by the cathode and its specific capacity and operating potential depends on the type of active material used as cathode.

The electrochemical reactions thus occurring in RMBs are as follows:[18]

Anode: $Mg \rightarrow Mg^{2+} + 2e^-$

Cathode: $Mg^{2+} + 2e^- + [Q] \rightarrow Mg[Q]$

Like every other energy storage device, operation of RMBs is initiated with charging and it completes with discharging. The charging/discharging in RMBs involves the movement of Mg ions which can be illustrated as:

Charging:

To facilitate the charge storage, Mg ions generated from the anode containing Mg compound. These Mg ions use the electrolyte as the conducting medium to transport cations from anode and embed into cathode.

Discharging:

Upon ejection from cathode, Mg ions utilize the electrolyte as the transporting/ionic conducting medium and diffuse through the separator to reach the anode. Hence Mg is again 'electroplated' back onto the anode.

During these charging/discharging states, electrons released flow through the external circuit thereby creating the electric current. In order for the RMBs to be commercialized, these charging/discharging process should be reversible over hundreds/thousands of cycles; thus, each of the above components require high levels of mechanical and electrochemical stability.

3. Currently used anodes for rechargeable Mg batteries

3.1. Mg metal anodes

As discussed earlier, pure Mg is considered as the dendrite free material when tested as an anode to rechargeable batteries. Though this assumption may not be true in all cases, the nature of dendrite formation is linked to the high reactiveness of the Mg metal creating instability at the anode and decomposition of the electrolyte. Recent studies showed that this dendrite formation is more severe than that of Li anodes in LIBs where the formation of dendrite layer at the electrode/electrolyte interface aides the diffusion of electrolyte ions and reduces the electrolyte decomposition during Li electroplating. Moreover, the strong polarizing nature of Mg^{2+} cations can result in interferences of Mg anodes and electrolytes. Lu et al[19] studied the correlation between morphology, surface chemistry and electrochemical behavior of Mg electrodes in polar aprotic solvents. In his studies, he observed a kind of passive film formation in aprotic solvents which blocked the transport of Mg^{2+} ions towards the electrode surface. Hence, continuous efforts are in progress to improve the compatibility of Mg anodes with the different electrolytes.

Several attempts have been made in the recent years to prevent the passivation of Mg anodes with the electrolytes. As shown in Figure 2A, Son et al[20] developed a new method to engineer conductive Mg^{2+} artificial interphase on the surface of Mg metal anode. This method allowed reversible plating/striping of Mg in oxidation resistant electrolytes while still restricting the electrolyte decomposition. The electrochemical performance of artificially coated Mg^{2+} anode and V_2O_5 cathode delivered 140 mA h g^{-1} specific capacity in water-based propylene carbonate (PC) electrolyte. The reason for this enhanced performance with increased potential window is attributed to the reduction in desolvation energy of Mg^{2+} in water and restricted coulombic repulsion between the host surface and Mg^{2+} ions. Additionally, the artificially conducting Mg^{2+} layer on the metal surface facilitates the use of oxidation resistant electrolytes like carbonate-based solutions without passivating Mg metal.

Recently, Zhang et al[21] dissolved $GeCl_4$ in ether electrolyte which acted as an ion-exchange agent to form artificial Ge protection layer on the Mg anode surface as indicated in Figure 2B. This process enabled the replacement of Mg atoms on the metal surface with Ge via galvanic exchange reaction of $Ge^{4+} + Mg \rightarrow Ge + Mg^{2+}$. Moreover, the assembles full cell with TiS_2/ Ti_3C_2 cathode delivered a capacity of 87.8 mA h g^{-1} at 10 mA g^{-1} current density over 30 cycles in Ge modified electrolyte. Additionally, the Mg anode with Ti_3C_2@CTAC cathode showed reversible capacity of ~100 mA h g^{-1} even at high current density of 50 mA g^{-1} indicating superior cyclic performance. The formation of Ge layer on metallic Mg acted as a protective layer preventing the formation of Mg^{2+} passivating layer and providing conducting passage for Mg electroplating in salt based organic electrolytes. Lv et al[22] treated Mg foils with $SnCl_2$-DEM solution forming an artificial Sn-based protective film via ionic-exchanging and alloying reactions. This artificial Mg_2Sn alloy composite enhanced the ionic transport kinetics whereas the insulated $MgCl_2/SnCl_2$ bestowed the much-needed potential gradient to prevent the electrolyte decomposition near the electrode surface. The artificially modified Mg anodes facilitated stable deposition/striping process over 4000 continuous life
cycles at 6 mA cm^{-2}.

The growth in material science and technology enabled the synthesis of Mg nano-powders with high specific surface area SSA) and pore volume which plays a crucial role in enhancing the electrochemical behavior. In this regard, Li et al[23] prepared the mesoporous Mg with spherical, rod like, sea-urchin like and plate like nanostructures via vapor-transport mechanism as shown in Figure 2C and studied their storage performance. The electrochemical analysis on the prepared structures proved that the energy density of Mg/air battery with sea-urchin nanomaterial retained 54% of its energy density even at 50 mA cm^{-2} current density. The rich porous network with high surface area sea-urchin Mg nanostructures reduced the polarization of Mg electrode thereby improving the rate capability and energy density. Similarly, Liang et al[24] synthesized ultra-small nano-sized Mg with 2.5 nm average diameter and used them as an anode for Mg batteries. The synthesized Mg anode with graphene/MoS_2 cathode displayed a discharge capacity of 170 mA h g^{-1} within a potential window of 1.8 V and the battery retained 95% of its capacity after 50 plating/stripping cycles. These studies proved that the use of high surface area Mg nanostructures might not completely mitigate the problem of dendrite formation but lead to thinner passivating film whereas the interconnected porous network

reduces the polarization and enhances the ion-transport kinetics of Mg ions during the cell operation.

3.2. Other metallic anodes and their alloys

Since the success of LIBs is mainly attributed to the use graphite anodes instead of Li metal, it is quite possible that RMBs which use Mg metal could be replaced with Mg ion insertion anodes that provides similar outcome. The driving force behind Mg-ion type insertion anodes is that it reduces the passivation of Mg metal on the anode surface and also provides reversible magnesiation/de-magnesiation in a variety of electrolytes. Although the exact nature of this behavior is unknown, one possible explanation might be ascribed to the thermodynamics of Mg ions in host matrices i.e., higher electrochemical potentials could make this happen than magnesium itself.[25]

Inspired by the LIBs, several combinations of metallic anodes and their alloys have been explored as anodes for RMBs. Table 2 shows the different types of alloy anodes investigated for RMBs along with their electrochemical characteristics. Among the alloy anodes, Bi and Sn are the most attractive alloy anode materials for RMBs. In this regard, Zhao et al[26] modified the surface of Mg metal anode with an artificially developed bismuth (Bi) protecting layer employing an ion-exchange interaction between bismuth trichloride ($BiCl_3$) and Mg metal. Interfacial characterization and electrochemical analysis demonstrated that the artificial Bi layer suppressed the passivation of Mg to a greater extent in non-corrosive $Mg(TFSI)_2$/DME electrolyte during continuous Mg striping/plating. The assembled full battery with $MgCu_{2-x}S$ and $Mg(TFSI)_2$/DME electrolyte showed a specific capacity of 210 mA h g^{-1} and over potential of ~0.4 V at a current density of 20 mA g^{-1}. Moreover, the battery maintained 52.3% of its capacity at high current density of 400 mA g^{-1}. Tin (Sn) is studied as another attractive anode material for Mg^{2+} insertion but its capacity has not been fully realized due to the interfacial anode-electrolyte reactions leading to irreversible capacity loss. Hence further investigation on reaction mechanism and design of Sn anodes is required to mitigate the capacity loss at the anode-electrolyte interface. Recently Song et al[27] studied the effect of downsizing bulk Sn into Sn nanoparticles to improve the (de)magnesiation kinetics as shown in Figure 3A. The electrochemical performance of these downsized Mg_2Sn anode investigated in 0.5 M $Mg(TFSI)_2$/THF showed a low capacity of 182 mA h g^{-1} in its first cycles but it's capacity has been greatly enhanced to 270 mA h g^{-1} after 15 cycles which can be ascribed to high surface to volume ratio of downsized Mg_2Sn nanoparticles obtained using ball-milling which lead to the decrease in Mg^{2+} diffusion length. On the other hand, Ikhe et al[28] reported the use of $3Mg/Mg_2Sn$ anode comprising of intermetallic Mg_2Sn, crystalline Mg-rich (c-Mg) and amorphous Mg-rich (a-Mg) phases. Here c-Mg is first de-alloyed in Mg $(HMDS)_2$: $MgCl_2$ (HMDS= hexamethyldisilazide) in the initial discharge process. The high SSA and pore volume caused the c-Mg to dissolve completely during the first cycle, whereas a-Mg and intermetallic Mg_2Sn are then de-magnesiated at slightly greater potentials leading to a discharge capacity of 1243 mA h g^{-1} (3.9 Mg^{2+}) at 100 mA g^{-1}. Moreover, the anode retained a capacity of 678 mA h g^{-1} without any trace of c-Mg reformation over 170 charge discharge cycles indicating the

excellent reversible Mg^{2+} plating/striping. Furthermore, de-alloying of $3Mg/Mg_2Sn$ anode with $Mg(HMDS)_2$: $MgCl_2$ makes it compatible with an array of conventional electrolytes.

Even though, Bi and Sn based anodes showed excellent capacities, they suffer from poor reversibility and slow transport kinetics of divalent Mg^{2+} ions. Hence, use of interfacial design is considered as a profound strategy to boost the ionic diffusion since phase/grain boundaries acts as a channel for faster diffusion of ions into the particle. Designing bi-phase or multi-alloy anodes is a smart strategy to create high density phase/grain boundary regions rather than single phase anode materials. In this regard, Niu et al[29] designed a dual phase nano-porous Bi-Sn alloy with high concentration of grain boundaries via a chemical Mg de-alloying of Mg–Bi–Sn precursors as shown in Figure 3B. Taking the advantage of its nanoporous structure and high surface area, the multi alloy Bi-Sn as anode of RMBs demonstrated superior charge storage performance than single phase counterparts. They examined various Bi-Sn contents and the optimized Bi_6Sn_4 electrode showed high specific capacity (434 mA h g^{-1}at 50 mA g^{-1}) and capacity retention (362 mA h g^{-1} at 1000 mA g^{-1}). Moreover, the electrode showed excellent long term stability (280 mA h g^{-1} after 200 cycles) with an efficiency of 99% after 30 cycles. According to ex-situ X-ray diffraction and morphological studies, Mg and Bi first reacted with each other during the first stage of magnesiation whereas the unreacted Sn phase functioned as a buffer matrix to suppress volumetric expansion. This is followed by Mg_3Bi_2 as a buffer matrix to further prevent the volume expansion as the Mg reacted with Sn. Mg_2Sn and Mg_3Bi_2 were converted to smaller Bi and Sn nanocrystals during the first de-magnesiation stage. Similarly, Sn and Mg_3Bi_2 served as buffer matrices to reduce volume shrinkage. Furthermore, the enlarged phase/grain boundaries offered a rapid Mg^{2+} diffusion channel. The enlarged phase/grain boundaries together with nanoporous structure facilitated additional channels for fast Mg^{2+} transport and shortened diffusion lengths for ion transport, thereby responsible for the Bi-Sn alloys better electrochemical performance. The same group also developed eutectic-like Bi-Sn layer with interdigited phase boundaries and nanostructured framework using single stage magnetron co-sputtering process. When compared to single phase pure Bi and Sn, the sputtered Bi-Sn film outperforms them in terms of their electrochemical performance with high discharge capacity (538 mA h g^{-1} at 50 mA g^{-1}) and cyclic performance of 233 mA h g^{-1} over 200 continuous discharge cycles. The bimetallic phase distribution of interdigitated Bi-Sn along with its porous structure and dual-phase buffer matrices synergistically enhances the ionic transport channels, shorten the diffusion paths, and restrict the volumetric changes thereby making the sputtered Bi-Sn films best anodes for superior magnesium storage performance.[30] In this way, these recently developed strategies offers valuable insights for developing high performance anodes for RMBs.

In summary, research on rechargeable Mg storage has been greatly improved over the past ten years with the evolution and optimization of new materials, but various aspects still needs to be investigated before these anodes can be used. For example, magnesium metal anodes exhibits certain remarkable electrochemical features, but its usage as an anode material has been found to be impractical, mostly due to its extraordinarily high sensitivity to surface reactions, which makes the selection of the electrolyte highly challenging. One must also note that the slow diffusion of magnesium ions results in sluggish electrode kinetics thereby impeding its

electrochemical performance.Indeed, the literature on Li-ion batteries provides some insights to overcome the sluggish electrode kinetics, some of which could be applied to Mg insertion anodes. On the other hand, insertion anodes attracted great interest because of its ability to adopt to general and well-known electrolytes that facilitate reversible magnesiation/de-magnesiation. However good cathode materials that are compatible with insertion anodes should be developed to interact with the electrolyte solution in a reversible manner. Although alloy based anodes such as Bi, Sn, etc., are studied as the alternate anodes for RMBs, they suffer from sluggish Mg^{2+} kinetics and substantial volume change during the plating/stripping process in conventional electrolytes. Hence, efforts should be made to overcome the slow electrode kinetics by altering the morphology or by reducing particle size which might enhance the performance of alloy anodes to some extent. To conclude this section, high capacity, good rate capability, excellent long term stability with high Coulombic efficiency are requirements of perfect anode material. More possible anode materials will need to be developed in the future, and alloy-based materials might result in the creation of a cutting-edge electrode material.

4. Recent developments in cathode materials

Like other battery materials, cathode materials play a vital role in the energy storage behavior of RMBs. For any material to be used as cathodes, it should satisfy the following properties: (i) high working potential and discharge capacity;(ii) quick and reversible insertion/extraction of Mg^{2+} ion (iii) excellent cyclic stability. Studies on rechargeable Mg battery cathodes are gaining traction these days in order to increase fundamental battery parameters such as voltage, capacity, and cycle life. Aurbach et al[47] reported the first prototype of Mg battery that included a Mg anode, Mo_6S_8 Chevrel phase (CP) cathode, and an organohaloaluminate salt electrolyte solution. The performance of this Mg battery prototype system is unsatisfactory owing to the reduced operating voltage (1.1 V). With the inspiration from the first prototype developed by Aurbach, several combinations of cathodes are experimented in the last two decades. Based on the charge storage mechanism, cathode materials used in RMBs are categorized as intercalation and conversion type cathodes. In this review, a quick overview on the major developments in the field of cathodes are described.

4.1. Intercalation type cathodes

Intercalation type cathodes retain their structural integrity during the continuous charge/discharge process, ensuring excellent cycle stability. Moreover, intercalation type cathodes provide high operating voltage which is essential in enhancing the energy density of the batteries. Intercalation type cathodes are further classified into Chevrel phase materials, layered materials, Prussian blue analog (PBA) and polyanionic cathode materials. The electrochemical performance of some of the important intercalation type cathode materials explored for RMBs has been summarized in Table 3.

4.1.1. Chevrel Phase (CP) cathode

Nowadays, the bulk of Li-ion rechargeable battery cathodes utilize intercalation/de-intercalation chemistry to store the charge. Similar kin of mechanism has been employed to study the cathode materials for RMBs. Despite the fact that various materials were tested, only

one group of materials known as Chevrel Phase displayed high rate capabilities with remarkable stability. CP also termed as ternary molybdenum chalcogenides $M_XMo_6T_8$ (M = Mg, Li, Zn, Na, T = S, Se, Te), exhibit excellent superconducting qualities and the ability to leach and replace some cations in the crystal structure, allowing for a wider range of applications based on chemical properties.

The Mo_6X_8 cluster makes up the CP structure as shown in Figure 4: six molybdenum atoms packed firmly together are contained within a nearly regular cubic cage. Eight chalcogen atoms (S, Se, Te), forming a so-called unit referred to as a "cluster" Within the cluster, the Mo–Mo distance is ~2.65–2.80. The $Mg_xMo_6S_8$ crystal structure ($0 \leq x \leq 2$) can also be seen as a Mo_6S_8 stacking. There is a maximum of 12 possible lattice sites (six-fold position) where the inner sites and others are formed at close proximity to the unit-cell origin and the outer sites form a ring around the inner places. Around the unit-cell, there are atoms between each pair of two blocks. Because of the charge transformation from Mg^{2+} to Mo or S atoms, the intercalated metal changes the spacing between the Mo atoms. It was estimated that a maximum of four electrons are transferred per Mo_6S_8 cluster as a result of which two bivalent Mg^{2+} cations are inserted at the origin. Saha et al[49] proposed a two-stage solution chemistry approach to manufacture unique cuboidal shaped $Cu_2Mo_6S_8$ Chevrel phase crystals with an average size of 1-1.5 μm. The electrochemical performance of Mo_6S_8 CP, produced by acidic leaching of Cu from $Cu_2Mo_6S_8$, demonstrated excellent cycling performance with high discharge capacity (76 mA h g^{-1} at ~C/6 rate) and rate capability. Moreover, the assembled prototype 2016-coin cell with Mo_6S_8 CP cathode exhibited a 66 mA h g^{-1} capacity at 1.5 C rate. Moreover, the full cell showed highest Coulombic efficiency of 99.3% at ambient temperature which is significantly higher than the previous reports. The unique solution chemistry approach is simple, and can likely be scaled-up for commercial applications. In other instance, Kim et al[50] offered two methods for improving Mo_6S_8 Mg storage performance. In first method, Cu was electrochemically reacted with Mo_6S_8 and in situ formed $Cu_xMo_6S_8$, the presence of nano-size Cu crystallites enhances the reversible capacity of Mo_6S_8. Furthermore, excellent cycling performance without any significant capacity loss was observed after 30 cycles by adding the Cu nanoparticle/graphene composite. The other alternative is to mechanically mill the Chevrel Mo_6S_8 powder into smaller particles, which can give shorter Mg^{2+} diffusion lengths, resulting in increased rate capabilities, and the sub-microsized CP has a larger reversible capacity than the microsized CP. In this way, a number of viable strategies for improving CP has been proposed including particle size reduction, using higher conductivity selenides rather than sulfides, and the incorporation of Cu into CP.

In summary, chevrel-phase Mo_6T_8 (where T = S, Se) is the most advanced cathode material for RMBs with the best intercalation kinetics because of its relatively open structure with many intercalation sites and shorter ion diffusion paths. Moreover, the presence of Mo_6 clusters, which have polarizable electron clouds that can effectively protect the host lattice from the highly charged Mg^{2+} ions. Despite the fascinating features, CP cathodes suffer from low working voltage vs Mg/Mg^{2+} which is only suitable for lower energy density applications. Hence future research should focus on raising the working voltage and energy density CP cathodes for RMBs.

4.1.2 Two dimensional (2D) layered materials

The layered material possess 2D transmission channels and acts as active hosts for Mg^{2+} ions. Their higher electron conductivities greatly improve the kinetics of Mg^{2+} ions, hence boosting Mg storage capacity. Layered transition metal oxides (MoO_3, V_2O_5), layered transition metal sulphides (MoS_2), and layered transition metal carbides (Ti_3C_2, V_2C, Ti_2C) etc. are some of the explored cathode materials for RMBs.

Figure 5A shows the crystal structure of vanadium pentoxide (V_2O_5), the widely used layered transition metal oxide consisting of layered polyhedral matrix structure. Novak et al[54] demonstrated the electrochemical insertion of Mg^{2+} in V_2O_5 employing 1 M Mg $(ClO_4)_2$ +1 M H_2O in acetonitrile. Their studies showed highest capacity of 170 A h kg^{-1} but the capacity quickly faded after 20 cycles. Fu et al[55] synthesized orthorhombic V_2O_5 nanowires using hydrothermal method and utilized them as cathode for RMB. The full cell with V_2O_5 nanowires as cathode, $Mg_xMo_6S_8$ (x=2) as anode and 1 M $Mg(ClO_4)_2$/AN as ionic medium exhibited a discharge capacity of 103 mA h g^{-1} /110 mA h g^{-1} in its first cycle. Moreover, high discharge capacity of 130 mA h g^{-1} was achieved in the sixth cycle at C/20 rate suggesting that the open tube structure with enhanced interlayer spacing improved the transport kinetics of Mg^{2+} ions. The energy storage performance of V_2O_5 cathode can also be improved by doping them with carbon materials and conducting polymers. Imamura et al[56] studied the Mg^{2+} insertion property in V_2O_5/carbon composite and found that the V_2O_5/carbon composite enhances the interlayer spacing and reduces the diffusion lengths compared to normal V_2O_5 xerogel. An et al[57] demonstrated the usage of graphene-decorated vanadium pentoxide aerogel as a cathode material for RMBs. The graphene-V_2O_5 composite shown in Figure 6A exhibited a reversible capacity of 330 mA h g^{-1} and retained 81% capacity after 200cycles. This performance can be attribute to the nanocomposite structure, which provided a two-way path for electrons/ions. Also, the crystal water in the aerogel induces a charge-shielding effect which accelerates the Mg^{2+} insertion into the electrode while the porous nature of graphene/V_2O_5 aerogel permits the electrolyte to easily enter the active material. Additionally, Miao et al[58] used in-situ polyaniline (PANI) polymerization to tailor the interlayer spacing of layered V_2O_5 nanosheets. The V_2O_5/PANI nanosheets demonstrated excellent Mg^{2+} intercalation/de-intercalation with high reversible capacity (361 mA h g^{-1}) at 20 mA g^{-1}. The excellent performance of V_2O_5/PANI nanosheets can be related to the enlarged interlayer spacing of V_2O_5 as a result of the PANI intercalation, which provides excess storage sites for Mg^{2+}. Moreover, the conjugated chains of PANI are responsible for insulating the electrostatic interactions between V_2O_5 and Mg^{2+} ions, which benefits the diffusion kinetics in RMBs. Recently, tuning the oxygen vacancies in the crystalline host of V_2O_5 cathode materials has recently been shown to improve electrochemical properties of cathode materials by providing ample surface-active sites and enhances the diffusion rate for ions storage. In this regard, Zhao et al[59] prepared bi-functional honeycomb like Ti-V_2O_{5-x} cathode material with abundant oxygen vacancies which showed high capacity of 241.3 mA h g^{-1} at 100 mA g^{-1} and maintained 195.4 mA h g^{-1} even after 400 cycles with good Coulombic efficiency. According to the ionic diffusion coefficient and electronic conduction analyses, the presence of oxygen vacancies can increase V_2O_5 intrinsic electrical conductivity while also improving Mg^{2+} transport kinetics inside the cathode, resulting in good

high-rate performance. This research suggests that defect engineering can help to enhance the electrochemical behavior of cathode materials for RMBs.

Layered Molybdenum oxide (MoO_3) is another well-known cathode material consisting of layered structure which is particularly advantageous for Mg^{2+} ion insertion and extraction. Its double layers are made up of edge and corner-sharing octahedrons [MoO_6] with weak van der Waals interaction as shown in Figure 5B. Gershinsky et al.[60] studied the Mg^{2+} intercalation in V_2O_5 and MoO_3 layered structures and found that MoO_3 cathode delivered 220 mA h g^{-1} discharge capacity with 95% efficiency in 0.1 M $MgTFSI_2$/AN electrolyte. Furthermore, Jacobson et al[61] showed that the oxide $Mo_{2.5+y}VO_{9+\delta}$ with 3D microporous framework delivered 397 mA h g^{-1} capacity [Figure 6B] during the first cycle, equating to 3.49 Mg^{2+} ions embedded in each unit. The dual effect of Mo and V can result in more than one oxidation state which facilitate charge redistribution and minimize volume expansion after Mg^{2+} ion insertion, preserving electro neutrality.

As shown in Figure 5C, Molybdenum disulfide (MoS_2) possess layered structure where two anion layers are sandwiched with one Mo cation layer by weak van der Waal interconnections[53], and it's been one of the most investigated RMB cathode materials. Han et al[62] employed hydrothermal process to synthesize defective MoS_2 nanosheets. They observed that the defective MoS_2 nanosheets showed high reversible capacity (152 mA h g^{-1}) and conductivity (R_{ct} = 2000 Ω) compared to defect free MoS_2. The use of pure MoS_2 is plagued by the smaller interlayer spacing which effects the transport kinetics of Mg^{2+}. Many efforts were made experimentally to increase the interlayer spacing by doping MoS_2 with carbon-based materials similar to metal oxides. In this regard, Tan et al[63] reported the formation of nanosheet like MoS_2 on nitrogen doped carbon nanofibers (N-CNFs) which showed a specific capacity of 131 mA h g^{-1} at 200 mA g^{-1} after 120 discharge cycles in LiCl-APC and $MgCl_2$-LiTFSI dual electrolyte. Similarly, sandwich-structured MoS_2/C microspheres was prepared by Liu et al[64] using hydrothermal method as shown in Figure 6C. These sandwich type composite structures showed superior electrochemical performance in RMBs with high initial discharge capacity and strong cycling stability. The synergistic interaction between the graphene-like structure and MoS_2 improves the electronic conductivity of MoS_2 allowing the rapid transport of Mg^{2+} ions. Moreover, existence of graphene improves the interplanar spacing of MoS_2 thereby enhancing the reversible Mg^{2+} plating/striping greatly. Liu et al.[65] employed lithium-assisted sonication method to prepare 3D Graphene like MoS_2/graphene with expanded interlayer distance of 0.98 nm. The unique MoS_2/graphene hybrid can efficiently improvee the electronic/ionic transport rate, provide a large number of active intercalation sites for Mg ions, and maintained its structural integrity throughout the cycling process. This unique architecture resulted in high capacity (115.9 mA h g^{-1}) and strong cyclic stability (82.5 mA h g^{-1} after 50 cycles) which is significantly better than that of bulk MoS_2 and bare graphene. Recently, Li et al.[66] prepared a ternary composite comprising MoS_2@C@PANI nanocomposite which showed a stable capacity of 114 mA h g^{-1} at 100 mA $^{-1}$ even after 100 cycles. It was also observed that the ternary cathode maintained a capacity of 105 mA h g^{-1} even at –5 ºC which indicates its potential for use under cold conditions. From these studies, it might be possible to use MoS_2-

based materials in RMBs because of the simple and scalable preparation process as well as excellent electrochemical performance.

MXenes belong to a family of transition metal carbides or nitrides and garnered lot of interest since their discovery in 2011. Because of their high SSA, excellent conductivity, and mechanical stability, MXenes have been widely used in energy storage devices such as LIB and supercapacitors because they can preserve their layered structure following multiple intercalation/de-intercalation operations. There have been few experimental studies on MXenes that have been applied to RMB to date. A one-step hydrothermal process was used to make a MoS_2/Ti_3C_2 composite with 165 mA h g^{-1} discharge capacity at 50 mA g^{-1}, high rate capability.[68] Very recently, Zhu et al[67] synthesized 3D interwoven Ti_3C_2 MXene using bacterial cellulose (BC) and utilized them as electrodes for RMBs. The presence of bacterial cellulose crumples the Ti_3C_2 flakes resulting in the creation of more electrolyte storage vacancies and also enhances the ionic Mg diffusion in-between the layers as shown in Figure 6D. The as prepared cathode material showed high discharge capacity (171 mA h g^{-1} at 50 mA g^{-1}) and maintained 88% of its initial capacity after 100 continuous cycles as shown in Figure 6E. Despite the fact that MXenes have intriguing electrochemical characteristics, their usage in ESDs is restricted because of its restacking nature during the continuous cycling process. In order to limit the restacting, MXenes sandwiched by carbon nanospheres (MXenes@C) were synthesized and tested as cathodes for magnesium batteries by Fan et al[69] using a self-assembling process. The MXenes@C heterostructure is created by electrostatic interactions between positively polarized 3D carbon nanospheres and negatively polarized 2D MXene nanosheets, which successfully enlarges the interlayer spacing and prevents MXene nanosheets from stacking back together, resulting in increased ion transport and shorter ion diffusion path. The MXenes@C [$Ti_3C_2T_x$@C nanospheres] cathode material demonstrated an excellent capacity of 198.7 mA h g^{-1} at 10 mA g^{-1} with 85% of its capacity retention after 400 cycles. These findings suggest that substantially more cathode materials for RMBs are possibly available, given the wide range of MXenes.

To conclude this section, we have outlined the current developments in layered materials for RMBs, including sulfides, oxides and MXenes. It can be observed from this review that compared to layered oxides, layered sulphides and Mxenes have superior structural stability. But, the oxides showed higher practical energy density and are more appealing to RMBs. We also discussed the methods investigated to promote the electrochemical behavior of the layered materials, such as adding water to the electrolyte or structure, widening the interlayer distance, reducing particle size, functionalizing with carbon materials, etc. The following areas need more study in order to address the demand for layered cathode materials in practical applications. First, it is vital to develop novel layered cathode materials that have excellent electrochemical performance, great abundance, simple synthesis route, and have a high structural stability. Second, in order to gain comprehensive knowledge of the Mg storage process in layered cathode materials, it is crucial to combine modern characterisation techniques with DFT calculations. Future studies must be focussed on enhancing the rate performance and cyclic stability of the existing layered cathode materials. For practical applications, it is necessary to develop high-performance layered cathode materials that can be produced on wider scale at a reasonable cost.

4.1.3. Prussian blue analogs (PBA)

Metal-organic framework (MOFs) with tunable and open crystal framework are known as Prussian blue analogues. The crystal structure of PBA was represented using the formula $A_xPR(CN)_6.yH_2O$, where A stands for interstitial alkali ions or water, while P, R stand for metal ions. Large interstitial A sites in the stable and open framework enable for kinetically facile and quick ion insertion and removal. As a result, this material has a long cycle life and can function at a high rate. In electrochemical investigations, the most frequent Prussian blue analogues are hydrated copper hexacyanoferrate and nickel hexacyanoferrate whose crystal structure are shown in Figure 7A and Figure 7B respectively.[70, 71] Mizuno et al[70] utilized copper hexacyanoferrate (CuHCF) PBA for the plating/stripping of Mg^{2+} ions using aqueous electrolytes. Excellent rate capability was attained thanks to the rapid transfer of hydrated Mg^{2+}, the discharge capacity reached up to 50 mA h g^{-1} at 0.1 A g^{-1} current density. In the presence of Na^+ ions, Kim et al[72] discovered $Na_{0.6}9Fe_2(CN)_6$ PBA that permits reversible plating/stripping of Mg^{2+} whereas Yagi et al[73] measured the redox potential of CuHCF PBA [Figure 7A] at a redox potential of 3V vs Mg/Mg^{2+} under aqueous and organic conducting mediums. Using a NiHCF as PBA cathode, a polyamide anode, and Mg^{2+} aqueous electrolyte, Chen et al[74] developed an aqueous Mg-metal battery with NiHCF cathode and polyimide anode which exhibited 1.5 V cell potential and stable cycle performance for 5000 cycles as shown in Figure 7D. On the other hand, Hong et al[75] demonstrated potassium nickel hexacyanoferrate (KNF-086) as a cathode material for RMBs using organic electrolyte. The cell exhibits a reversible plating/stripping of Mg^{2+} ions, with reversible capacity of 48.3 mA h g^{-1} [as shown in Figure 7C] at a 0.2 C rate and 2.99 V discharge voltage (vs. Mg/Mg^{2+}), which is the highest of any cathode material yet recorded for RMBs. Wang et al[76] and his group reported a new kind of PBA- carbon composite $NaV_2O_2(PO_4)_2F/rGO$ as a material for Mg^{2+} ion insertion. This new kind of cathode material demonstrated excellent discharge voltage of 3.3 V vs Mg^{2+}/Mg and the assembled Mg- full cell displayed energy and power density of 76 W h kg^{-1}, 1300 W k g^{-1} in organic electrolyte as shown in Figure 7E. It has been observed that the diffusion energy barriers of Mg^{2+} have found to be efficiently reduced using 1D continuous diffusion channels and fluorophosphate with little steric hindrance. Furthermore, the presence of F^- can improve the operating voltage by increasing the electronegativity of $(PO_4)^{3-}$.

Although, these studies prove that PBAs have the potential to operate under aqueous as well as organic electrolytes with long term stability and high rate performance, there are still a number of issues that must be resolved before they can be commercialised, including lower coulombic efficiency, poor cycling life, and low discharge capacity. The poor electrical conductivity of PBAs was a significant obstacle to their commercialization. The primary technique to solve this problem is modification using various carbonaceous materials such as graphene, carbon black and carbon nanotubes. Future PBA synthesis will include a variety of modification techniques in an effort to enhance the electrochemical behavior of PBAs on all fronts. Finally we hope that fresh perspectives will aid in the continued advancement of PBA cathodes for highly efficient RMBs.

4.1.4. Polyanion compounds

Polyanion compounds are formed via firm covalent interactions between polyanions and transition metals, with 3D network topologies. These materials have a wide range of properties, including high working potentials and mechanically stable structure, making them viable cathodes for RMBs. Polyanionic compounds are primarily silicates with olivine structures silicates and phosphates with NASICON structures. The theoretical capacity and theoretical redox potential of olivine-type $MgMSiO_4$ (M = Mn, Ni, Fe, or Co) are very high and the existence of multivalent transition metals might have less impact on its structure which is caused by Mg^{2+} ion de-intercalation. In light of the aforementioned advantages, a number of nanoparticles with shorter diffusion paths, such as $MgMnSiO_4$[77], $Mg_{1.03}Mn_{0.97}SiO_4$[78], $MgFeSiO_4$[79], and 3D heterogeneous porous $MgCoSiO_4$[80], have been investigated as possible hosts for Mg ions. When compared to bulk forms, electrochemical analysis suggests that $MgCoSiO_4$ with a mesoporous structure had greater peak currents, a large discharge capacity, long cycle life, and superior rate capability. It's believed that the narrow pore walls in $MgCoSiO_4$ decreased the transportation path for both ions and electrons, whereas the greater surface area gave more active sites for redox reactions to take place. Orikasa et al[81] studied the electrode kinetics of $MgFeSiO_4$ produced by electrochemical ion exchange of Li_2FeSiO_4 was greatly improved. To put it another way, $2Li^+$ extraction from Li_2FeSiO_4 was followed by Mg^{2+} insertion, resulting in $MgFeSiO_4$ with a capacity of over 300 mAh g^{-1} and good cycling retention. These findings will serve as a benchmark for improving the use of PBAs as magnesium battery electrodes in the future.

4.1.5 Other cathode materials

Unlike the previously mentioned intercalation cathodes, titanium dioxide (TiO_2) has been investigated as one of the cathode material because of its rapid ions storage, large capacity. The use of anatase-phase TiO_2 as cathode for RMBs has been investigated by Zhang et al[82] in phenyl complex electrolyte (APC), showing only 80 mAh g^{-1} at 5 mA g^{-1}. Both spectroscopic and microscopic approaches show that a Mg:Ti ratio of 0.1:1 can be electrochemically or chemically injected into anatase TiO_2 without phase transition. Strasser et al[83] used aliovalent doping to increase the titanium vacancies which serves as intercalation vacancies. The introduction of aliovalent doping lead to the enhancement in Mg ion storage in anatase TiO_2, and the discharge capacity rose from 25 mAh g^{-1} to 140 mAh g^{-1} at 20 mA g^{-1} current density. The uniform distribution of these vacancies is thought to provide a network of diffusion channels for high-valent cations to diffuse between these vacancy sites. Despite the fact that aliovalent doping improved performance, managing the chemical reaction of these vacancies is extremely challenging. As a result, new strategies for increasing TiO_2 magnesium storage are needed. Cai et al[84] doped anatase ultrafine TiO_2 nanocrystals with carbon and employed them as a cathode material for Mg metal batteries. The Arrhenius behavior showed that the activation energy of carbon doped TiO_2 (TiO_2-UN@C) has been significantly reduced compared to the undoped TiO_2 (TiO_2-UN) suggesting the improvement ion migration of TiO_2 nanocrystals with carbon framework (Ti-MOF). The schematic of energy storage in Ti-MOF was shown in Figure 8A. As shown in Figure 8A, $MgCl^+$ and Mg^{2+} are injected into TiO_2-UN@C at a depth of several nanometers below the material surface for the discharge process whereas Ti(IV) in TiO_2 nanocrystals, undergoes faradaic reaction and changes into Ti (III). Thus, both the surface-controlled and faradaic processes contribute to the high reversible capacity and cyclic stability

to the system. 2D $VOPO_4$ nanosheets with enlarged interlayer spacing (1.42 nm) are manufactured by ultrasonic exfoliation and self-assembling. The increase in interlayer distance enables sufficient 2D diffusion channels for $MgCl^+$ ion flow with low polarization. Benefiting from its expanded interlayer spacing, Mg battery with 2D $VOPO_4$ nanosheets as cathode, Mg as anode displayed a remarkable capacity of 310 mA h g^{-1} at 50 mA g^{-1} and excellent cyclic stability as shown in Figure 8B.[85] Wang eta al. analyzed the effect of water on the transport kinetics of Mg ions in $VOPO_4$ cathodes. Electrochemical tests shown in Figure 8C proved that the water in the electrolyte will equilibrate with the structural water in the $VOPO_4$ lattice, reduces the diffusion between electrode/electrolyte interface and enhances the transport kinetics for electrochemical intercalation of Mg-ions in $VOPO_4$.[86] Figure 8D shows the SEM image of interconnected sea-urchin-like VS_4 nanodendrites are generated using a surfactant-assisted solution-phase method. Benefitting from its chain-like crystalline structure, large specific surface area and weak van-der Waals forces (shown in Figure 8E), abundant active sites are provided for Mg^{2+} plating/stripping with improved electrode kinetics. Moreover, the structural integrity VS_4 atomic chains are well retained, ensuring outstanding reversibility and cycling life of the Mg–VS_4 battery.[87] On the other hand, Li et al[88] developed VS_4@Ti_3C_2/C nano-micro structures by electrostatic self-assembly and hydrothermal method. Excessive magnesium storage sites were exposed thanks to the strong V-C bond that held VS_4 nanosheets securely to Ti_3C_2. High reversible capacity of 492 mA h g^{-1} at 50 mA g^{-1} and great cycling performance (more than 900 cycles at 500 mA g^{-1}) was obtained because of its unique nano-micro framework.

Because of its superior electrochemical behavior with a well-defined plateau at 3.4 V (vs. Na^+/Na) and excellent rate capability, [$Na_3V_2(PO_4)_3$ (NVP)] Na-superionic conductor (NASICON) is recognized as the most promising cathode for energy storage devices. As shown in Figure 8F, the NASICON type materials is made by corner sharing VO_6 octahedra with PO_4 tetrahedra in 2:3 ratio (known as "lantern"). In the rhombohedral crystal, two types of interstitial sites (6b and 18e) exist; three Na^+ per formula unit are allotted in both sites with a ratio of (Na1):(Na2) 1:2. The two Na^+ at the 18e site can be extracted with regard to the charging plateau at 3.4 V (vs. Na^+/Na), yielding $NaV_2(PO_4)_3$, with only the 6b site remaining to maintain structural integrity.[89, 90] A simple spray drying - annealing procedure was used to make mesoporous NVP/C spheres. After removing two Na ions from the NVP/C cathode, the desodiated electrode ED-NVP/C was tested as an insertion host for Mg^{2+} ions. The ED-NVP/C electrode showed a discharge potential of 2.5 V (vs. Mg^{2+}/Mg), with an excellent cycle stability and reversible capacity of 88.8 mA h g^{-1} at 20 mA g^{-1} as shown in Figure 8G.[91] The electrochemical characteristics of the desodiated $Na_3V_2(PO_4)_3$ cathode in $Mg(BF_4)_2$-based electrolyte has been tested by Hayashi et al.[92] Although, the NVP electrode suffered from polarization during the discharge, the electrode delivered a discharge plateau of ~2.7 V (vs Mg^{2+}/Mg) with an excellent discharge capacity >100 mA h g^{-1} at room temperature. These findings pave the path for researchers to investigate alternative NASICON-structured cathode materials for RMBs.

Even one and half decades after the first prototype by Aurbach, research on magnesium batteries is still in its infancy, despite its great promise as high energy density storage media. The apparent lack of a suitable cathode that could combine with Mg anode in a useful

electrochemical device is one of the main obstacles in Mg battery research. There is currently no perfect combination of materials that completely fits the requirements for high energy density, acceptable recyclability, and excellent cyclic stability despite the fact that a number of materials have been reported to be active as Mg battery cathodes. Hence, significant innovations are still required in the field of cathodes for RMBs before they can be commercialized.

4.2. Conversion type cathode materials

The multiple electron transfer and large theoretical capacity makes conversion-type electrodes an inexpensive and promising cathode for RMBs. Their thermodynamically stable conversion reaction might bypass the sluggish Mg^{2+} plating/stripping, making it a viable alternative to intercalation type cathode materials. The structural reorganizing and chemical bond breaking during the redox reactions enables the conversion type cathode to work with full capacity, and these changes are highly reversible in nature. Because of these features, the Mg^{2+} insertion/extraction of conversion type cathode materials will be several orders higher than the intercalation counterparts. Sulfides and redox-active organic compounds are commonly used as conversion type cathode materials. Some of the latest studies on conversion type cathodes are collated, along with their reported specific capacity values in Table 4.

4.2.1. Redox active organic compounds

Employing carbonyl functional groups (C=O) as an active host for Mg^{2+} ions. Redox active organic compounds have attracted huge interest in the recent times. However, the high polarizing nature of Mg^{2+} ions causes the structural damage leading to the capacity loss during the plating/stripping process. Considering the above stated issues, the storage capacity of organic compounds can be enhanced through doping, organic polymer polymerization, and electrolyte optimization.

Pan et al[94] investigated the use of 2,5-Dimethoxy-1,4-benzoquinone (DMBQ) as a cathode material to host Mg^{2+} ions in magnesium-based electrolytes. The reported material showed excellent storage capacity of 319 mA h g^{-1} with a potential window slightly greater than 2.0 V vs Mg/Mg^{2}+ in Mg $(TFSI)_2$. $MgCl_2$ in DME electrolyte. However, the capacity quickly faded due to the electrode dissolution phenomena upon cycling. The same group also prepared three types of anthraquinonyl-based polymers shown in Figure 9A and tested as organic cathodes for RMBs. Among the three cathode materials, 26PAQ (2,6-Polyanthraquinone) and 14PAQ (1,4-Polyanthraquinone) exhibited better cathode performance but the capacity of 26PAQ quickly faded due to its rigid polymer chain network. Whereas, the redox active Quinone groups of 14-PAQ are situated on one side of the polymer chain providing rotational flexibility to the organic polymer chains. In compared to 26PAQ, this rotational adaptability helps eliminate space impediment and softens the stress induced on the polymer structure, resulting in greater structure stability for 14PAQ. These structural advantages resulted in less capacity loss during the initial stage but the capacity remained stable in the next hundreds of cycles as shown in Figure 9B.[95] Figure 9C shows the schematic of Mg/EV battery developed by Sun et al.[96] The Mg cathode based on ethyl viologen (EV), not only possess quick redox couple EV^{2+}/EV° but also couples with redox-active anions like iodide (I), allowing for entire four-electron storage.

Due to its intrinsic fast electrode kinetics, the redox pair $EV^{2+}/EV°$ has a better rate capability (10 C) and a longer life span (500 cycles). At a rate of 1.0 C and a high material loading of 5 mg cm^{-2}, a high material utilization (>80%) can be attained. Moreover, the redox reactions are highly reversible in nature with four electron storage, high gravimetric energy density of 304.2 W h kg^{-1} and the without any capacity fluctuations over 100 cycles is achieved when coupling with iodide. This research shows how to create reversible multiple-electron storage for developing high rate and high energy RMBs.

To conclude, there is a lot of promise for using organic compounds as a high performance cathodes for RMBs. By using molecular design and synthetic techniques, the main shortcomings of organic compounds, such as their high solubility and poor electrical conductivity, might be overcome. The unique advantage of organic electrodes for RMBs is their structural variety and ability to tailor the electrochemical properties by changing the chemical structure. This offers a fantastic opportunity to get around some fundamental Mg-ion transport limitations and create high-performance cathode materials for RMBs.

4.2.2. Sulfide materials

Because of the high theoretical capacity (1671 mA h g^{-1}) of sulfur, combining Mg anode with sulfur (S) cathode is gaining traction. The dual effect of Mg metal anode and Sulfur cathode renders Mg-S battery with 1.77 V theoretical potential and specific energy 1722 W h kg^{-1} and 3200 W h L^{-1}, respectively. Moreover, the two-electron redox reaction in the form of $Mg^{2+} + S + 2e^- \rightleftarrows MgS$ makes Mg-S batteries potential candidate for high energy density storage device.[97] Muldoon et al[98] developed the first rechargeable Mg-S battery using sulfur cathode, Mg metal anode and non-nucleophilic hexamethyldisilazide magnesium chloride and aluminum trichloride [HMDSMgCl-$AlCl_3$] electrolyte. The as-prepared coin-cell type Mg-S battery showed high discharge capacity of 1200 mA h g^{-1} during the initial cycle with a starting potential of 0.55 V. But the capacity of the Mg-S coin-cell quickly faded even though the potential increased to 0.89 V during the second discharge cycle. The decay in specific capacity was attributed to the sulfur dissolution in the electrolyte which was clearly explained by X ray photoelectron spectroscopic (XPS) studies. The oxidation state of sulfur shifted to lower energy levels dramatically during the first discharge cycle which was ascribed to migration of polysulfide in between the cathode and anode via a shuttling mechanism. This research laid foundation in the development of non-nucleophilic electrolyte compatible with an electrophilic sulphur cathode.[98] The cycling stability of Mg-S batteries can be improved by doping sulfur with carbon-based materials. Fichtner et al[99] developed Mg-S battery with graphene-sulfur composite as cathode [as shown in Figure 10A] which displayed high discharge capacity of 448 mA h g^{-1} and maintained 52.6% of its capacity after 50 discharge cycles indicating excellent cyclic stability. The use of graphene-sulfur as cathode proved to be successful because graphene acts as a buffer layer which allows minimum volume fluctuations during reversible cycling between sulphur and MgS while also providing high electrical conductivity and a large surface area for active material dispersion. Similarly, pre-activated carbon nanofiber (CNF) loaded with sulfur material as cathode and CNF coated separator enhanced the discharge capacity of Mg-S

battery with high discharge capacity of 1200 mA h g^{-1} without any considerable decay after 20 cycles.[100]

In the search for sulfur-based cathode materials, transition metal sulfides (TMS) such as titanium sulfide (TiS_3), cobalt sulfide (CoS) and copper sulfide (CuS) has shown significant potential for Mg^{2+} intercalation/de-intercalation. CuS is a hexagonal layered transition metal sulfide (LTMS) with an interlayer distance of 8.2 nm. Because of its inexpensive cost, abundant resources, great theoretical discharge capacity of 560 mA h g^{-1}, and high electronic conductivity (103 S cm^{-1}), it has been shown to be efficient electrode for LIBs and sodium-ion batteries.[101] Reduced particle size and better morphologies are two strategies for increasing reversible capacity. Xu et al[102] prepared hollow CuS nanocubes and used them as cathodes for RMBs. The hollow structured CuS nanocubes shown in Figure 10B demonstrated excellent reversible capacity of 200 mA h g^{-1} at 100 mA g^{-1} and remarkable cyclic stability. Similarly, Nanostructured CuS delivered a specific capacity of 300 mA h g^{-1} in $Mg(ClO_4)_2$/AN and 175 mA h g^{-1} in $Mg(HMDS)_2$-$AlCl_3$ electrolyte with excellent durability. Due to the lower diffusion length and increased SSA, nanostructured CuS favored reversible insertion of Mg-ions into CuS matrix without any rapid aggregation leading to excellent cyclic stability.[103, 104] On the other hand, Cao et al[105] in 2019 employed microwave assisted route to prepare CuS nanosheets as cathode material for Mg battery. The electrochemical testing results demonstrated that CuS nanosheets as cathode material exhibited a discharge capacity of 300 mA h g^{-1} at 20 mA g^{-1} current density (Figure 10C) and the device showed excellent rate capability (237.5 mA h g^{-1} at 100 mA g^{-1}), cyclic stability (135 mA h g^{-1} at 200 mA g^{-1} over 200 discharge cycles). The unique structural design of CuS nanosheets effectively increases the contact area between the electrolyte and the electro-active material, provides abundant reactive sites to improve electron/ion transport properties, and allows for sufficient volume expansion during the continuous cycling process. Enhancing the interplanar distance proved to be an effective approach to increase the electron transport properties of cathode materials. In this regard, Shen et al[106] used CTAB to enhance the interlayer distance of CuS material and used them as a cathode for Mg storage which showed excellent energy storage of 415 W h kg^{-1} at 50 mA g^{-1} in non-corrosive Mg ion electrolyte. In their work, CTAB was used to enlarge the interlayer distance of CuS which resulted in higher specific surface area as shown in Figure 10D. The CuS conversion cathode as constructed, provides remarkable extended cycling stability over 1000 cycles [Figure 10E] because of the interlayer expansion that promotes Mg-ion insertion/extraction and improved electrochemical compatibility with the electrolyte. CuS cathode research has made significant progress since the publication of the initial study by Nazar et al[107] in 2016. However, CuS-based cathodes frequently experience drastic phase transformation, significant structural collapse, and substantial volume change due to high lattice strain and mechanical stress. This leads to delayed reaction kinetics, which limits the reaction degree and cycle life. Phase engineering is considered as an effective method for controlling the crystal structure and chemical composition of copper sulphide cathodes for battery application. Cao et al[108] and his group creared a non-stoichiometric-phase stable $Cu_{7.2}S_4$ nanotubes with mixed valence and many lattice defects using a microwave-induced selective etching technique. Under 100 mA g^{-1} current rate, $Cu_{7.2}S_4$ nanotubes delivered high specific capacity of 314 mAh g^{-1} and good rate capability of 91.7 mAh g^{-1} under 1000 mA g^{-1}. With

acutely low discharge capacity degradation of 0.0109% per cycle, the $Cu_{7.2}S_4$ nanotubes delivered stable performance over 1600 cycles demonstrating excellent cycling stability. This research proposes that a high-performance rechargeable magnesium battery cathodes may be accomplished through defect engineering, structure controlling, and phase strategy. Regulating the anionic chemistry of cathode materials can improve the redox reversibility and electrode kinetics of the cathode materials. Additional anions with a higher ionic radii and polarizability can be introduced to modify the host lattice structure and create a better channel for Mg^{2+} ion transport. Nevertheless, the effect of anionic chemistry is poorly understood, and anionic Te-substituted CuS cathode has only been documented in a few cases. Cao et al[109] employed anionic Te-substitution strategy to enhance the reversible Cu^0/Cu^+ redox reactions in Te-substituted $CuS_{1-x}Te_x$ nano-sheet cathodes. X-ray absorption fine structure analysis showed that the Te dopants substitute the anionic sites of sulphur atoms, resulting in an enhanced oxidation state of the Cu species. The kinetically stable $CuS_{1-x}Te_x$ (x = 0.04) nanosheets delivered a reversible capacity of 446 mA h g^{-1} at 20 mA g^{-1} and excellent cyclic stability with 0.0345% per cycle at 1 A g^{-1}. These studies demonstrate that anionic substitution strategy plays a significant role in regulating the cathode chemistry allowing researchers to investigate the potential of rechargeable magnesium batteries.

Due to its excellent electrochemical properties, CoS has been studied extensively in dye-sensitized solar cells, supercapacitors and alkaline batteries. The use of nanoflower like CoS as conversion cathode for RMB was first reported by Ding et al[110]. The flower like structures (shown in Figure 10F) with ~40 nm thickness showed a discharge capacity of 150 mA h g^{-1} at 50 mA g^{-1} but the capacity reduced considerably at higher current density due to the sluggish diffusion kinetics of Mg^{2+} ions in solid state. Nevertheless, these research gives insight into the novel cathode materials like CuS and CoS as a new platform for hosting Mg^{2+} ions in the bulk and at interfaces which apparently contribute to the evolution of new Mg positive electrode materials. For RMBs, TiS_3 is another promising conversion cathode. Arsentev et al[111] examined the electrochemical characteristics of Mg in layered TiS_3 model system. When Mg was intercalated from the electrolyte, an exothermic phase transformation occurred and the calculations revealed a shift in layers, as well as a change in Mg coordination to trigonal prismatic from square pyramidal. As the proportion of Mg rises, the S–S bonds in the disulfide ion are broken, and TiS_3 layers are converted to ribbons. The resulting phase is metastable, decomposing readily and irreversibly into MgS and TiS_2 as shown in Figure 10G. The most difficult task in developing a reversible TiS_3-based cathode is suppressing this breakdown. In the [010] direction, an extremely low migration barrier of 0.292–0.698 eV was discovered which is substantially lower than the 0.8–1.2 eV of layered and spinel TiS_2 which proves that TiS_3 can be successfully employed as cathode for RMBs. Other class of materials that have been tested as conversion anodes for RMBs are selenium sulfide (SeS_2) and nickel sulfide (NiS_x).[112, 113] The reports on the performance of these materials are very few and will require further research. Hence sulfides act a promising Mg^{2+} hosts and further research should be carried out understanding divalent ion diffusion in lattices and Mg desolvation at the electrolyte/electrode interface.

Finally to conclude, variety of sulfide materials such as copper sulfide, cobalt sulfide, titanium sulfide, and tungsten sulfides have been investigated as cathode materials for RMBs. Even though transition metal sulfides showed excellent electrochemical performance towards the Mg^{2+} deposition/stripping, there is still have a long way to go before they can be used as active cathode materials in the RMBs. First, it is necessary to look into how cathode materials affect the mechanism of MIBs and the factors that affect kinetic delay. Finding innovative approaches to develop TMS with enhanced electrochemical performance is required because various forms of transition metal sulfides have various crystal structures. Second, to accelrate the transport kinetics of Mg^{2+} ions, transition metal sulfides with enhanced interlayer spacing should be developed. Thirdly, transition metal sulfides can be doped with other 2D materials such as graphene, Mxenes which not only improves the electronic conductivity but also provides structural (mechanical) stability. In light of this, we anticipate that this study will provide a clear framework and specific approaches for future practical and theoretical research on the creation of high-performance transition metal sulfides for RMBs.

5. Electrolytes

As shown in the schematic Figure 1, the electrolyte plays a vital part in transporting ions within the two electrodes. Low corrosivity, wide working voltage window, superior ionic conductivity, and reversible Mg plating/striping are all desirable characteristics for a RMB electrolyte. Moreover, electrolytes should agree with the safety features such as less volatile, less toxic and inflammable. The electrolytes in RMBs are broadly categorized as aqueous and solid-state electrolytes. According to their nature and physical state, we review and present these electrolytes in the following subsections. The characteristics of sample electrolytes are listed in Table 1 according to their categories.

5.1. Aqueous electrolytes

Grignard-based electrolytes, boron-containing electrolytes, and $(HMDS)_2Mg$-based electrolytes are the three main types of aqueous electrolytes.

5.1.1. Grignard-based and $(HMDS)_2Mg$-based electrolytes

Grignard-based electrolytes prevents the formation of passivation layer while allowing for reversible magnesium transfer. The electrolyte's properties are found in the R group, with chemical composition of RMg_x (R corresponds to alkyl/aryl groups and X=Cl, Br, or other halides) where different configuration will provide different outcomes.[114] The first prototype of RMB reported by Aurbach used $Mg(AlCl_2R)_2$/tetrahydrofuran (THF) as the electrolyte but it's application was precluded due to its lower working potential of 2.2 V vs Mg/Mg^{2+} on Pt. They then created a high-voltage stable all-phenyl complex (APC) electrolyte which provided large working potential (>3.0 V vs Mg/Mg^{2+} on Pt), specific conductivity of 2×10^{-3} S cm^{-1}, less over potential, and cycling efficiency approaching 100%.[115] The ionic mobility and anodic stability have greatly been improved by mixing Grignard electrolytes with ionic liquids. This phenomenon has been observed by Lee et al[116] where a series of charge-transport species with high chemical stability are formed by combining Grignard reagent with allyl-functionalized ionic liquid. On the other hand, $(HMDS)_2Mg$-based ionic conductive agents were proposed as

viable alternatives for the implementation of Mg-S batteries with non-nucleophilic characteristics, excellent anodic stability, and compatibility with high-voltage cathodes like Sulphur. Gao et al[117] used lithium salt LiTFSI [lithium bis(trifluoromethanesulfonyl)imide] as an additive to develop Mg/S battery. The $(HMDS)_2Mg$-LiTFSI electrolyte could combine reversible Mg^{2+} plating/striping with sulfur cathode via Li^+ ions which stimulates the inactive MgS and MgS_2. The cell exhibited excellent discharge capacity of 1000 mA h g^{-1} even after 30 cycles and a significant energy density of 874 W h kg^{-1}. Even though $(HMDS)_2Mg$ based electrolytes showed promising features, the cost of these electrolytes is a significant disadvantage.

5.1.2. Boron-based electrolytes

Extensive attempts have been made to construct effective halogen-free RMB electrolytes based on boron-centered anions since early findings from Gregory et al showed that Mg organo-borates [$Mg(BPh_2Bu_2)_2$ or $Mg(BPhBu_3)_2$] were compatible with Mg anodes.[118] Boron chemistry is fascinating because it acts as an electron acceptor and can easily form polyanionic compounds by coordinating with electron-rich nucleophiles. Boron-based electrolytes also alleviate the corrosion problem that Grignard and $(HMDS)_2Mg$-based electrolytes had, which was caused by the presence of chlorine (Cl), and can accomplish reversible Mg plating/stripping, making it a feasible non-corrosive electrolyte for RMBs. In 2012, Guo et al[119] reported the use of tri(3,5-dimethylphenyl) borane (Mes_3B) and PhMgCl to make Mes_3B-$(PhMgCl)_2$ electrolytes which showed excellent electrochemical properties with wide anodic potential, ionic conductivity, and high cyclic stability. It was understood that the excess PhMgCl and the probable stable active species: Mes_3BPh, $MgCl^+$, $Mg_2Cl_3^+$, and Mg-Cl moieties resulted in a non-covalent interaction between $[Mes_3BPh]^-$ anions and $(PhMgCl)_2$ that enhanced the electrochemical characteristics. But the performance quickly faded since the electrodes on the other hand were corroded by the halogen. Mohtadi et al[120] reported the use of halide free $Mg(BH_4)_2$ as an inorganic salt for Mg plating/stripping in ether solvents (THF and DME). The inclusion of $LiBH_4$ to $Mg(BH_4)_2$/DME resulted in significant increase in coulombic efficiency and current density when tested with Chevrel phase (Mo_6S_8) cathode. Despite its poor oxidative stability (1.7 V vs. Mg on platinum), the electrolyte's reversibility in the absence of halides and THF distinguishes it for the development of a new class of $Mg(BH_4)_2$-based electrolytes. Cui et al[121] presented a new BMOC electrolyte prepared via. single step dissolution method. The BMOC electrolyte has excellent anodic stability (up to 4.2 V vs. Mg), strong reversibility for Mg plating/stripping. Furthermore, the BMOC electrolyte is free of corrosive effects on traditional metallic current collectors, and its compatibility with the sulphur cathode suggests that it has a promising future in rechargeable Mg-S battery systems. Besides, Oh et al[122] prepared Al-compatible boron electrolyte by dissolving Mg metal powder in ethereal solution containing tris(2H-hexafluoroisopropyl)borate (THFPB) and 1,2-dimethoxyethane (DME). The electrolyte showed excellent electrochemical stability (3.5 V vs Mg/Mg^{2+}) and high reversibility when tested with Mo_6S_8 or S_8 cathodes and several current collectors. Zhu et al[123] developed a new type of halogen-free boron based electrolyte ($Mg[Mes_3BPh]_2$/THF) which showed a high ionic conductivity of 1.5×10^{-3} S cm^{-1}) and good Mg plating/stripping for rechargeable Mg batteries. Aurbach et al[124] employed electrochemical “conditioning” step to

eliminate the unwanted moieties in Mg[B(hexafluoroisopropanol)$_4$]$_2$/dimethoxyethane (Mg[B(HFIP)$_4$]$_2$/DME) electrolyte. The use of electrochemical "conditioning" process removes all the acidic and atmospheric contaminants from the Mg[B(HFIP)$_4$]$_2$/DME thereby enhancing the current density, overpotential for Mg plating/stripping (3.0 - 3.2 V vs Mg/Mg^{2+}) and cyclic efficiency. Despite the fact that the fundamental nature of the conditioning process is not fully understood, future work should involve a fundamental analysis of the process, with a focus on spectroscopic measurements, as well as optimization and scale-up of the approach.

Magnesium salts based on carba-closo-borate anions have been investigated as potentially useful supporting electrolytes in ethers, with the probability to expand the potential window. Mohtadi et al[125] was the first to report Mg(CB$_{11}$H$_{12}$)$_2$/tetraglyme (MMC) electrolyte, which had a high anodic stability (3.8 V vs Mg) and excellent compatibility with Mg metal, non-corrosive. Following that, Lavallo et al[126] and Zavadil et al[127] reported the use of carborane anions (such as CB$_{11}$H$_{11}$F$^-$, HCB$_9$H$_9^-$) and achieved reversible Mg intercalation/de-intercalation with high Coulombic efficiency and a wide electrochemical window. McArthur[126] in 2016 developed a novel and cost-effective method for producing halide-free electrolytes for RMBs, which involves chemically reducing reactive cations with the metal Mg. To create a electrochemically stable monocationic electrolyte 1[MgR^{1+}] with an organic ligand, a unique comproportionation approach was established between diorganomagnesium reagent and halide-free Mg salt with weakly coordinating carborane anion 1[Mg^{2+}]. With an oxidative stability of 4.6 V vs. Mg$^{0/2+}$, this new electrolyte demonstrated a significant potential for reversible Mg deposition and desolution.To conclude, boron-based electrolytes are by far the most attractive electrolytes for RMBs due to their superior electrochemical characteristics, and these breakthroughs pave the path for non-corrosive boron-based electrolytes for large-scale production of RMBs.

In conclusion, a variety of aqueous electrolytes with distinctive properties have been tested as an electrolyte for reversible magnesium plating/stripping. Grignard-based electrolytes possess good Coulombic efficiency and low overpotential, but the poor anodic stability and undesirable chemical reactivity towards the cathodes prevent them for real time battery applications. Similarly, boron based electrolytes suffer from restricted solubility and very low anodic stability, high reactivity. Although the (HMDS)$_2$Mg-based electrolyte has good electrochemical performance, their high cost has become an obstacle for their large-scale applications. Despite the broad electrochemical window of a carbaborate anions-based electrolyte, extensive study and application are constrained by the expensive raw materials. One should also note that electrolyte pre-treatment is frequently required since impurities like H_2O are unavoidable in aqueous Mg electrolytes, however electrolyte pre-treatment does not compensate for good reversibility and low over-potential. This problem still stands in the way of RMBs having a robust, long-lasting metal electrode-electrolyte interface. New electrolyte designs may offer the possibility of high purity and, thus, excellent compatibility with magnesium anodes.

5.2. Solid-state electrolytes

Solid-state electrolytes have gained traction recently due to its numerous benefits, including good mechanical stability, larger operating potential, high volumetric energy density and safe to operate. They are classified as inorganic, organic, and organic-inorganic composite

electrolytes. Among them, inorganic electrolytes didn't get much attention because of their lower electronic conductivity whereas organic solid-state electrolytes made by combining Mg salt and complex organic polymers have high ionic conductivity, excellent cyclic stability and lower degree of polarization which is an essential parameter for RMBs. Polyethylene oxide (PEO), polyvinylidene fluoride-hexafluoropropylene (PVDF-HFP), polyvinylidene fluoride (PVDF), polyvinyl alcohol (PVA) are widely used polymer host matrices. Recently, Sun et al[128] prepared a quasi-solid-state electrolyte composed of PVDF-HFP and nanosized $SiO_2MgTFSI_2$. The solid-state electrolyte has a strong ion conductivity (0.83 mS cm^{-1}), supports reversible Mg^{2+} plating/striping and is extremely compatible with the electrodes. After 100 cycles, the assembled full cell with a layered TiO_2 cathode demonstrate a high discharge capacity of 129 mA h g^{-1} (150 W h kg^{-1}) with no decline. The reason for this excellent performance is attributed to dynamic characteristic of a aqueous electrolyte with the superior stability of a solid-state electrolyte. Polymer electrolytes with inorganic fillers such as Al_2O_3, SiO_2, TiO_2, SiO_2, MgO make up the organic-inorganic electrolytes with high coulombic efficiency for Mg insertion/extraction and good long-term stability. A new type of organic-inorganic solid-state polymer electrolyte made up of PEO, magnesium borohydride $Mg(BH_4)_2$, and magnesium oxide (MgO) nanoparticles was first reported by Shao et al[129] The semitransparent PEO/Mg $(BH_4)_2$/MgO thin film electrolyte cells have a good Coulombic efficiency of Mg deposition/dissolution (98%) and excellent long term stability.

In summary, research on solid state Mg electrolytes are still in their early stage. Solid-state electrolytes should ideally possess the following properties: (i) wide potential window (ii) high thermal and chemical stability (iii) compatible with magnesium metal and high-voltage cathodes (iv) high ionic conductivity of Mg^{2+} in solid-state electrolytes (v) high mechanical strength (vi) easy preparation process in addition to being affordable, secure, and environmentally friendly. Future studies on solid state electrolytes should mainly focus on improving the electrochemical potential window without compromising its ionic conductivity and better oxidation stability. use of sophisticated characterization techniques to understand the mechanism of ion transport inside the polymer framework.

6. Conclusions and Future perspective

Magnesium batteries are still a hot topic of interest in their current state, with early prototypes created in labs all over the world. Despite its impressive performance, it is still out of range before being practically applicable due to the poor compliance between electrodes and electrolyte. The key to improve the performance of RMBs is to identify new types of electrode materials and to optimize the electrolyte system. This article briefly summarized the current progress made in terms of materialistic components (anodes and cathodes) and electrolyte solvents.

For anodes, mainly Mg metal and alternative alloy type anodes on Bi, Sn, Pb, In etc. are used. The majority of studies concentrate on the creation of advanced cathode materials due to the potential of using pure Mg as anode. The extensively researched Grignard-based electrolyte solutions can be used with pure Mg metal anodes but Mg metal suffers from passivation. Moreover, the Grignard-based electrolyte solutions, restricted by a small voltage window and

toxicity. Hence, alternative alloy type anodes such as Bi, Sn, Pb, In etc. have been investigated widely because they allow for reversible Mh plating/stripping in a wide range of electrolytes while also ensuring better compatibity with cathodes. Bi and Sn alloys showed favourable characteristics such as low reduction potentials, facile alloying reactions, and high discharge capacity. But they suffer from sluggish Mg^{2+} transport kinetics and volume contractions during magnesium plating/striping which prevents them from being employed in real systems at the moment. Furthermore, the alloy anodes considerably increase the anode potential, resulting in a very low working voltage and an increase in cost. Future perspective on alloy anodes could focus on improving the sluggish electrode kinetics by introducing high surface area nanomaterials of different morphologies which can enhance the transport kinetics of Mg^{2+} inside the anode, reduces the passivation of Mg on the anode as well as improves the cyclic stability. Due to their superior qualities when compared to Bi and Sn alone, dual-phase alloy anodes have been suggested by numerous groups as a potential solution. This is mostly because to their improved kinetics and high degree of reversibility. Hence, future research can be directed towards the multi-alloy anode materials with appropriate morphologies which can significantly reduce the volume contraction and improves the overall performance of the device. Despite fewer studies, insertion anodes such as Li_3VO_4 also demonstrated promising potential for Mg^{2+} plating/striping and this might be further enhanced by doping. Future studies on anodes can also be directed towards novel 2D materials such as Mxenes and graphene based materials. Although there is very little information on 2D materials used as RMB anodes, there is a lot of potential for these materials due to their distinctive layered structure and variable interlayer spacings.

For cathodes, we have summarized the recent developments on intercalation and conversion type cathode materials. Chevrel phase is regarded as the most promising intercalation cathode material for commercially feasible Mg ion batteries because of its high Mg ion diffusion rate, excellent electrical conductivity, and reversible Mg ion plating/stripping. However, Chevrel phase materials suffer from poor energy density and low discharge voltage plateau. Layered cathode materials (MoS_2, V_2O_5, MoO_3, etc.) showed great promise because of their good electrode kinetics and tunable interlayer spacing. While layered oxides showed high magnesium ion insertion voltage and higher energy density, which is more appealing to RMBs, layered sulphides and selenides demonstrated better structural stability. In this review, we summarized the successful methods investigated to improve the storage properties of the layered materials, such as adding water to the electrolyte and/or structure, widening the interlayer distance, adjusting the anionic chemistry, decreasing the particle size, and also doping with carbonaceous materials. As discussed in this review, very few layered materials have been used as cathode materials for RMBs till date, and future study should concentrate on the following areas. First, it is still crucial to create novel layered cathode materials that have excellent electrochemical performance, great abundance, facile synthesis at low cost, high structural stability. Second, in order to tailor the surface of layered intercalation cathodes for better interfacial electrode kinetics, a deeper knowledge of the charge transport kinetics at the cathode/electrolyte interface is required. Thirdly, explore new strategies to enhance the energy density, cyclic stability and rate kinetics of existing layered materials.

Among coversion type cathodes, we discussed about the recent developments in redox active organic compounds and sulfides which showed promising cathode features. As discussed in this review, redox active organic compounds (26PAQ, 14PAQ, and PAQS) have shown faster electrode kinetics due to the poor interaction between Mg^{2+} and organic molecules. However, their performance is constrained by severe dissolution and poor electronic conductivity. Since redox active organic compounds are structurally diverse and possess tunable chemical structure, more research into these materials presents a great opportunity to get around some fundamental Mg-ion transport limitations and create high-performance Mg batteries. For high-energy Mg-S batteries, sulfide (CuS, $Cu_{7.2}S_4$, $CuS_{1-x}Te_x$, TiS_3) cathodes with naturally favourable redox kinetics can be seen as a promising option. However, Mg anode passivation and electrolyte degradation are hindering Mg-S battery research because of the dissolution of polysilfide. Hence a thorough understanding of the chemistry occurring in Mg-S battery systems and the interactions at the electrode/electrolyte interface is vital for creating solutions to the performance limiting constraints.

As far as electrolytes are concerned, there is a lot of room for improvement in the Mg metal compatibility and electrochemical stability of electrolytes. Although, several advancements were made in the electrolytes such as Grignard-based, $(HMDS)_2Mg$-based and solid-state electrolytes, each electrolyte has its own set of benefits and drawbacks. Hence thorough understanding of the fundamental concepts such as interaction between Mg anode| Mg complex electrolyte solutions| high voltage cathode interfaces should be further investigated to achieve the compatibility between electrode and electrolyte solutions. Also, the scalability and commercial viability of these electrolytes is debatable since their preparation processes are quite complex, wherein the precursors themselves require non-trivial synthesis procedures. Hence in order to present RMBs as a sustainable alternative to LIBs, the electrodes and electrolyte should be composed of readily available precursors.

In conclusion, RMBs are still in the early phases of development compared to LIBs. Fortunately, there is still more untapped chemical space in the form of novel shapes and chemistries, which opens up the possibility of developing Mg anodes with reduced dendrite formation, practical cathodes with improved kinetics and higher energy densities and electrolytes with reversible Mg^{2+} plating/stripping and improved cyclic stability. We hope that this assessment will serve as a catalyst for researchers to work harder on developing RMBs as a viable storage device getting past LIBs.

Conflict of Interest

The authors declare that they have no competing financial interests or personal relationships that may have influenced the results reported in this paper.

Data Availability Statement

Data sharing is not applicable to this article as no new data were created or analyzed in this study.

References

1. Wang X, Weng Q, Yang Y, Bando Y, Golberg D. Hybrid two-dimensional materials in rechargeable battery applications and their microscopic mechanisms. Chemical Society Reviews. 2016;45(15):4042-4073.
2. Liang Y, Jing Y, Gheytani S, Lee K-Y, Liu P, Facchetti A, et al. Universal quinone electrodes for long cycle life aqueous rechargeable batteries. Nature materials. 2017;16(8):841-848.
3. Yang ZG, editor Electrochemical Energy Storage for Green Grid: Status and Challenges. ECS Meeting Abstracts;IOP Publishing. 2011;4:155.
4. Grey C, Tarascon J. Sustainability and in situ monitoring in battery development. Nature materials. 2017;16(1):45-56.
5. Ma Y, Shuai K, Zhou L, Wang J, Wang Q. Effect of Mg^{2+} and Mg^{2+}/Li^{+} electrolytes on rechargeable magnesium batteries based on an erythrocyte-like CuS cathode. Dalton Transactions. 2020;49(43):15397-15403.
6. Luntz A. Beyond lithium ion batteries. ACS Publications; 2015. p. 300-1.
7. Wu X, Leonard DP, Ji X. Emerging non-aqueous potassium-ion batteries: challenges and opportunities. Chemistry of Materials. 2017;29(12):5031-5042.
8. Sun R, Pei C, Sheng J, Wang D, Wu L, Liu S, et al. High-rate and long-life VS_2 cathodes for hybrid magnesium-based battery. Energy Storage Materials. 2018;12:61-68.
9. Massé RC, Uchaker E, Cao G. Beyond Li-ion: electrode materials for sodium-and magnesium-ion batteries. Science China Materials. 2015;58(9):715-766.
10. Erickson EM, Markevich E, Salitra G, Sharon D, Hirshberg D, de la Llave E, et al. Development of advanced rechargeable batteries: a continuous challenge in the choice of suitable electrolyte solutions. Journal of The Electrochemical Society. 2015;162(14):A2424.
11. Wang F, Fan X, Gao T, Sun W, Ma Z, Yang C, et al. High-voltage aqueous magnesium ion batteries. ACS central science. 2017;3(10):1121-1128.
12. Song J, Sahadeo E, Noked M, Lee SB. Mapping the challenges of magnesium battery. The Journal of Physical Chemistry Letters. 2016;7(9):1736-1749.
13. Slater MD, Kim D, Lee E, Johnson CS. Sodium‐ion batteries. Advanced Functional Materials. 2013;23(8):947-958.
14. Shah R, Mittal V, Matsil E, Rosenkranz A. Magnesium-ion batteries for electric vehicles: Current trends and future perspectives. Advances in Mechanical Engineering. 2021;13(3):16878140211003398.
15. Ponrouch A, Frontera C, Bardé F, Palacín MR. Towards a calcium-based rechargeable battery. Nature materials. 2016;15(2):169-172.
16. Wang N, Wan H, Duan J, Wang X, Tao L, Zhang J, et al. A review of zinc-based battery from alkaline to acid. Materials Today Advances. 2021;11:100149.
17. Elia GA, Kravchyk KV, Kovalenko MV, Chacón J, Holland A, Wills RG. An overview and prospective on Al and Al-ion battery technologies. Journal of Power Sources. 2021;481:228870.
18. Foot PJ. Principles and prospects of high-energy magnesium-ion batteries. Science Progress. 2015;98(3):264-275.
19. Lu Z, Schechter A, Moshkovich M, Aurbach D. On the electrochemical behavior of magnesium electrodes in polar aprotic electrolyte solutions. Journal of Electroanalytical Chemistry. 1999;466(2):203-217.
20. Son S-B, Gao T, Harvey SP, Steirer KX, Stokes A, Norman A, et al. An artificial interphase enables reversible magnesium chemistry in carbonate electrolytes. Nature Chemistry. 2018;10(5):532-539.
21. Zhang J, Guan X, Lv R, Wang D, Liu P, Luo J. Rechargeable Mg metal batteries enabled by a protection layer formed in vivo. Energy Storage Materials. 2020;26:408-13.

22. Lv R, Guan X, Zhang J, Xia Y, Luo J. Enabling Mg metal anodes rechargeable in conventional electrolytes by fast ionic transport interphase. National science review. 2020;7(2):333-341.
23. Li W, Li C, Zhou C, Ma H, Chen J. Metallic magnesium nano/mesoscale structures: their shape‐controlled preparation and Mg/air battery applications. Angewandte Chemie International Edition. 2006;45(36):6009-6012.
24. Liang Y, Feng R, Yang S, Ma H, Liang J, Chen J. Rechargeable Mg batteries with graphene‐like MoS_2 cathode and ultrasmall Mg nanoparticle anode. Advanced Materials. 2011;23(5):640-643.
25. Kuang C, Zeng W, Li Y. A review of electrode for rechargeable magnesium ion batteries. Journal of Nanoscience and Nanotechnology. 2019;19(1):12-25.
26. Zhao Y, Du A, Dong S, Jiang F, Guo Z, Ge X, et al. A Bismuth-based protective layer for magnesium metal anode in noncorrosive electrolytes. ACS Energy Letters. 2021;6(7):2594-2601.
27. Nguyen D-T, Song S-W. Magnesium stannide as a high-capacity anode for magnesium-ion batteries. Journal of Power Sources. 2017;368:11-17.
28. Ikhe AB, Han SC, Prabakar SR, Park WB, Sohn K-S, Pyo M. $3Mg/Mg_2Sn$ anodes with unprecedented electrochemical performance towards viable magnesium-ion batteries. Journal of Materials Chemistry A. 2020;8(28):14277-14286.
29. Niu J, Gao H, Ma W, Luo F, Yin K, Peng Z, et al. Dual phase enhanced superior electrochemical performance of nanoporous bismuth-tin alloy anodes for magnesium-ion batteries. Energy Storage Materials. 2018;14:351-360.
30. Song M, Niu J, Yin K, Gao H, Zhang C, Ma W, et al. Self-supporting, eutectic-like, nanoporous biphase bismuth-tin film for high-performance magnesium storage. Nano Research. 2019;12(4):801-808.
31. Benmayza A, Ramanathan M, Singh N, Mizuno F, Prakash J. Electrochemical and thermal studies of bismuth electrodes for magnesium-ion cells. Journal of The Electrochemical Society. 2015;162(8):A1630.
32. Shao Y, Gu M, Li X, Nie Z, Zuo P, Li G, et al. Highly reversible Mg insertion in nanostructured Bi for Mg ion batteries. Nano letters. 2014;14(1):255-260.
33. Liu Z, Lee J, Xiang G, Glass HF, Keyzer EN, Dutton SE, et al. Insights into the electrochemical performances of Bi anodes for Mg ion batteries using 25 Mg solid state NMR spectroscopy. Chemical Communications. 2017;53(4):743-746.
34. Tan Y-H, Yao W-T, Zhang T, Ma T, Lu L-L, Zhou F, et al. High voltage magnesium-ion battery enabled by nanocluster Mg3Bi2 alloy anode in noncorrosive electrolyte. ACS nano. 2018;12(6):5856-5865.
35. Penki TR, Valurouthu G, Shivakumara S, Sethuraman VA, Munichandraiah N. In situ synthesis of bismuth (Bi)/reduced graphene oxide (RGO) nanocomposites as high-capacity anode materials for a Mg-ion battery. New Journal of Chemistry. 2018;42(8):5996-6004.
36. Singh N, Arthur TS, Ling C, Matsui M, Mizuno F. A high energy-density tin anode for rechargeable magnesium-ion batteries. Chemical communications. 2013;49(2):149-151.
37. Nguyen DT, Tran XM, Kang J, Song SW. Magnesium storage performance and surface film formation behavior of tin anode material. ChemElectroChem. 2016;3(11):1813-1819.
38. Nguyen GTH, Nguyen DT, Song SW. Unveiling the Roles of Formation Process in Improving Cycling Performance of Magnesium Stannide Composite Anode for Magnesium‐Ion Batteries. Advanced Materials Interfaces. 2018;5(22):1801039.
39. Arthur TS, Singh N, Matsui M. Electrodeposited Bi, Sb and $Bi_{1-x}Sb_x$ alloys as anodes for Mg-ion batteries. Electrochemistry Communications. 2012;16(1):103-106.

40. Cheng Y, Shao Y, Parent LR, Sushko ML, Li G, Sushko PV, et al. Interface promoted reversible Mg insertion in nanostructured Tin‐Antimony Alloys. Advanced Materials. 2015;27(42):6598-6605.
41. Niu J, Yin K, Gao H, Song M, Ma W, Peng Z, et al. Composition-and size-modulated porous bismuth‐tin biphase alloys as anodes for advanced magnesium ion batteries. Nanoscale. 2019;11(32):15279-15288.
42. Song M, Zhang T, Niu J, Gao H, Shi Y, Zhang Y, et al. Boosting electrochemical reactivity of tin as an anode for Mg ion batteries through introduction of second phase. Journal of Power Sources. 2020;451:227735.
43. Murgia F, Weldekidan ET, Stievano L, Monconduit L, Berthelot R. First investigation of indium-based electrode in Mg battery. Electrochemistry Communications. 2015;60:56-59.
44. Murgia F, Monconduit L, Stievano L, Berthelot R. Electrochemical magnesiation of the intermetallic InBi through conversion-alloying mechanism. Electrochimica Acta. 2016;209:730-736.
45. Wang L, Welborn SS, Kumar H, Li M, Wang Z, Shenoy VB, et al. High‐Rate and Long Cycle‐Life Alloy‐Type Magnesium‐Ion Battery Anode Enabled Through (De) magnesiation‐Induced Near‐Room‐Temperature Solid‐Liquid Phase Transformation. Advanced Energy Materials. 2019;9(45):1902086.
46. Blondeau L, Foy E, Khodja H, Gauthier M. Unexpected behavior of the InSb alloy in Mg-ion batteries: unlocking the reversibility of Sb. The Journal of Physical Chemistry C. 2018;123(2):1120-1126.
47. Aurbach D, Lu Z, Schechter A, Gofer Y, Gizbar H, Turgeman R, et al. Prototype systems for rechargeable magnesium batteries. Nature. 2000;407(6805):724-727.
48. Levi E, Gershinsky G, Aurbach D, Isnard O, Ceder G. New insight on the unusually high ionic mobility in chevrel phases. Chemistry of materials. 2009;21(7):1390-1399.
49. Saha P, Jampani PH, Datta MK, Okoli CU, Manivannan A, Kumta PN. A convenient approach to Mo6S8 Chevrel phase cathode for rechargeable magnesium battery. Journal of The Electrochemical Society. 2014;161(4):A593.
50. Choi S-H, Kim J-S, Woo S-G, Cho W, Choi SY, Choi J, et al. Role of Cu in Mo_6S_8 and Cu mixture cathodes for magnesium ion batteries. ACS applied materials & interfaces. 2015;7(12):7016-7124.
51. Liu F, Song S, Xue D, Zhang H. Selective crystallization with preferred lithium-ion storage capability of inorganic materials. Nanoscale research letters. 2012;7(1):1-17.
52. Ma W, Alonso-González P, Li S, Nikitin AY, Yuan J, Martín-Sánchez J, et al. In-plane anisotropic and ultra-low-loss polaritons in a natural van der Waals crystal. Nature. 2018;562(7728):557-562.
53. Li X, Zhu H. Two-dimensional MoS2: Properties, preparation, and applications. Journal of Materiomics. 2015;1(1):33-44.
54. Novak P, Desilvestro J. Electrochemical insertion of magnesium in metal oxides and sulfides from aprotic electrolytes. Journal of The Electrochemical Society. 1993;140(1):140.
55. Fu Q, Sarapulova A, Trouillet V, Zhu L, Fauth F, Mangold S, et al. In operando synchrotron diffraction and in operando X-ray absorption spectroscopy investigations of orthorhombic V_2O_5 nanowires as cathode materials for Mg-ion batteries. Journal of the American Chemical Society. 2019;141(6):2305-2315.
56. Imamura D, Miyayama M. Characterization of magnesium-intercalated V_2O_5/carbon composites. Solid State Ionics. 2003;161(1-2):173-180.
57. An Q, Li Y, Yoo HD, Chen S, Ru Q, Mai L, et al. Graphene decorated vanadium oxide nanowire aerogel for long-cycle-life magnesium battery cathodes. Nano Energy. 2015;18:265-172.

58. Yang J, Miao X, Zhang C, Zheng J, Sun C, Zhang Y, et al. In‐Situ Lattice Tunnel Intercalation of Vanadium Pentoxide for Improving Long‐Term Performance of Rechargeable Magnesium Batteries. ChemNanoMat. 2022;8(4):e202200025.
59. Wu D, Zhuang Y, Wang F, Yang Y, Zeng J, Zhao J. High-rate performance magnesium batteries achieved by direct growth of honeycomb-like V_2O_5 electrodes with rich oxygen vacancies. Nano Research. 2021;6:1-8.
60. Gershinsky G, Yoo HD, Gofer Y, Aurbach D. Electrochemical and spectroscopic analysis of Mg2+ intercalation into thin film electrodes of layered oxides: V_2O_5 and MoO_3. Langmuir. 2013;29(34):10964-10972.
61. Kaveevivitchai W, Jacobson AJ. High capacity rechargeable magnesium-ion batteries based on a microporous molybdenum‐vanadium oxide cathode. Chemistry of Materials. 2016;28(13):4593-4601.
62. Zhu F, Zhang H, Lu Z, Kang D, Han L. Controlled defective engineering of MoS2 nanosheets for rechargeable Mg batteries. Journal of Energy Storage. 2021;42:103046.
63. Tan YH, Zhou F, Huang ZH, Yao WT, Zhang TW, Yao HB, et al. MoS_2‐Nanosheet‐Decorated Carbon Nanofiber Composites Enable High‐Performance Cathode Materials for Mg Batteries. ChemElectroChem. 2018;5(7):996-1001.
64. Liu Y, Jiao L, Wu Q, Du J, Zhao Y, Si Y, et al. Sandwich-structured graphene-like MoS_2/C microspheres for rechargeable Mg batteries. Journal of Materials Chemistry A. 2013;1(19):5822-5826.
65. Liu Y, Fan L-Z, Jiao L. Graphene intercalated in graphene-like MoS_2: A promising cathode for rechargeable Mg batteries. Journal of Power Sources. 2017;340:104-110.
66. Liu J, Zhong Y, Li X, Ying T, Han T, Li J. A novel rose-with-thorn ternary MoS_2@ carbon@ polyaniline nanocomposite as a rechargeable magnesium battery cathode displaying stable capacity and low-temperature performance. Nanoscale Advances. 2021;3(19):5576-5580.
67. Zhu J, Shi R, Liu Y, Zhu Y, Zhang J, Hu X, et al. 3D interwoven MXene networks fabricated by the assistance of bacterial celluloses as high-performance cathode material for rechargeable magnesium battery. Applied Surface Science. 2020;528:146985.
68. Xu M, Bai N, Li H-X, Hu C, Qi J, Yan X-B. Synthesis of MXene-supported layered MoS_2 with enhanced electrochemical performance for Mg batteries. Chinese Chemical Letters. 2018;29(8):1313-1316.
69. Liu F, Liu Y, Zhao X, Liu X, Fan L-Z. Pursuit of a high-capacity and long-life Mg-storage cathode by tailoring sandwich-structured MXene@ carbon nanosphere composites. Journal of Materials Chemistry A. 2019;7(28):16712-16719.
70. Mizuno Y, Okubo M, Hosono E, Kudo T, Oh-Ishi K, Okazawa A, et al. Electrochemical Mg^{2+} intercalation into a bimetallic CuFe Prussian blue analog in aqueous electrolytes. Journal of Materials Chemistry A. 2013;1(42):13055-13059.
71. Wessells CD, Peddada SV, Huggins RA, Cui Y. Nickel hexacyanoferrate nanoparticle electrodes for aqueous sodium and potassium ion batteries. Nano letters. 2011;11(12):5421-5425.
72. Kim D-M, Kim Y, Arumugam D, Woo SW, Jo YN, Park M-S, et al. Co-intercalation of Mg^{2+} and Na^+ in $Na_{0.69}Fe_2(CN)_6$ as a high-voltage cathode for magnesium batteries. ACS applied materials & interfaces. 2016;8(13):8554-8560.
73. Yagi S, Fukuda M, Ichitsubo T, Nitta K, Mizumaki M, Matsubara E. EQCM analysis of redox behavior of CuFe Prussian blue analog in mg battery electrolytes. Journal of The Electrochemical Society. 2015;162(12):A2356.
74. Chen L, Bao J, Dong X, Truhlar D, Wang Y, Wang C, et al. Aqueous Mg-ion battery based on polyimide anode and prussian blue cathode. ACS Energy Letters. 2017;2(5):1115-1121.

75. Chae MS, Hyoung J, Jang M, Lee H, Hong S-T. Potassium nickel hexacyanoferrate as a high-voltage cathode material for nonaqueous magnesium-ion batteries. Journal of Power Sources. 2017;363:269-276.
76. Wang J, Tan S, Zhang G, Jiang Y, Yin Y, Xiong F, et al. Fast and stable Mg^{2+} intercalation in a high voltage $NaV_2O_2(PO_4)_2F$/rGO cathode material for magnesium-ion batteries. Science China Materials. 2020;63(9):1651-1662.
77. Mori T, Masese T, Orikasa Y, Huang Z-D, Okado T, Kim J, et al. Anti-site mixing governs the electrochemical performances of olivine-type $MgMnSiO_4$ cathodes for rechargeable magnesium batteries. Physical Chemistry Chemical Physics. 2016;18(19):13524-13529.
78. Feng Z, Yang J, NuLi Y, Wang J. Sol‐gel synthesis of $Mg_{1.03}Mn_{0.97}SiO_4$ and its electrochemical intercalation behavior. Journal of Power Sources. 2008;184(2):604-609.
79. Heath J, Chen H, Islam MS. $MgFeSiO_4$ as a potential cathode material for magnesium batteries: ion diffusion rates and voltage trends. Journal of Materials Chemistry A. 2017;5(25):13161-13167.
80. Zheng Y, NuLi Y, Chen Q, Wang Y, Yang J, Wang J. Magnesium cobalt silicate materials for reversible magnesium ion storage. Electrochimica acta. 2012;66:75-81.
81. Orikasa Y, Masese T, Koyama Y, Mori T, Hattori M, Yamamoto K, et al. High energy density rechargeable magnesium battery using earth-abundant and non-toxic elements. Scientific reports. 2014;4(1):1-6.
82. Zhang M, MacRae AC, Meng YS, editors. Investigation of Anatase-TiO_2 As an Efficient Electrode Material for Magnesium-Ion Batteries. ECS Meeting Abstracts; 2016: IOP Publishing.2016;2:301.
83. Koketsu T, Ma J, Morgan BJ, Body M, Legein C, Dachraoui W, et al. Reversible magnesium and aluminium ions insertion in cation-deficient anatase TiO_2. Nature materials. 2017;16(11):1142-1148.
84. Cai X, Xu Y, An Q, Jiang Y, Liu Z, Xiong F, et al. MOF derived TiO_2 with reversible magnesium pseudocapacitance for ultralong-life Mg metal batteries. Chemical Engineering Journal. 2021;418:128491.
85. Zhou L, Liu Q, Zhang Z, Zhang K, Xiong F, Tan S, et al. Interlayer spacing regulated $VOPO_4$ nanosheets with fast kinetics for high‐capacity and durable rechargeable magnesium batteries. Advanced Materials. 2018;30(32):1801984.
86. Ji X, Chen J, Wang F, Sun W, Ruan Y, Miao L, et al. Water-activated $VOPO_4$ for magnesium ion batteries. Nano letters. 2018;18(10):6441-6448.
87. Wang Y, Liu Z, Wang C, Yi X, Chen R, Ma L, et al. Highly branched VS_4 nanodendrites with 1D atomic‐chain structure as a promising cathode material for long‐cycling magnesium batteries. Advanced materials. 2018;30(32):1802563.
88. Zhu J, Zhang X, Gao H, Shao Y, Liu Y, Zhu Y, et al. VS_4 anchored on Ti_3C_2 MXene as a high-performance cathode material for magnesium ion battery. Journal of Power Sources. 2022;518:230731.
89. Jian Z, Yuan C, Han W, Lu X, Gu L, Xi X, et al. Atomic structure and kinetics of NASICON $Na_xV_2(PO_4)_3$ cathode for sodium‐ion batteries. Advanced Functional Materials. 2014;24(27):4265-4272.
90. Song W, Ji X, Wu Z, Zhu Y, Yang Y, Chen J, et al. First exploration of Na-ion migration pathways in the NASICON structure $Na_3V_2(PO_4)_3$. Journal of Materials Chemistry A. 2014;2(15):5358-5362.
91. Zeng J, Yang Y, Lai S, Huang J, Zhang Y, Wang J, et al. A Promising High‐Voltage Cathode Material Based on Mesoporous $Na_3V_2(PO_4)_3$/C for Rechargeable Magnesium Batteries. Chemistry‐A European Journal. 2017;23(66):16898-16905.

92. Hasegawa G, Akiyama Y, Tanaka M, Ishikawa R, Akamatsu H, Ikuhara Y, et al. Reversible Electrochemical Insertion/Extraction of Magnesium Ion into/from Robust NASICON-Type Crystal Lattice in a Mg $(BF_4)_2$-Based Electrolyte. ACS Applied Energy Materials. 2020;3(7):6824-6833.
93. Kang G-S, Li S, Bhoraskar SV, Yoo J-B. Effect of the Crystalline Structure of $Cu_x Mo_6S_8$ on the Capacity of Mg-Based Secondary Batteries. ACS Applied Energy Materials. 2022;5(7):8346-8356.
94. Pan B, Zhou D, Huang J, Zhang L, Burrell AK, Vaughey JT, et al. 2, 5-Dimethoxy-1, 4-Benzoquinone (DMBQ) as organic cathode for rechargeable magnesium-ion batteries. Journal of The Electrochemical Society. 2016;163(3):A580.
95. Pan B, Huang J, Feng Z, Zeng L, He M, Zhang L, et al. Polyanthraquinone‐Based Organic Cathode for High‐Performance Rechargeable Magnesium‐Ion Batteries. Advanced Energy Materials. 2016;6(14):1600140.
96. Sun Y, Zou Q, Lu YC. Fast and Reversible Four‐Electron Storage Enabled by Ethyl Viologen for Rechargeable Magnesium Batteries. Advanced Energy Materials. 2019;9(48):1903002.
97. Aurbach D, Cohen Y, Moshkovich M. The study of reversible magnesium deposition by in situ scanning tunneling microscopy. Electrochemical and Solid-State Letters. 2001;4(8):A113.
98. Kim HS, Arthur TS, Allred GD, Zajicek J, Newman JG, Rodnyansky AE, et al. Structure and compatibility of a magnesium electrolyte with a sulphur cathode. Nature communications. 2011;2(1):1-6.
99. Vinayan B, Zhao-Karger Z, Diemant T, Chakravadhanula VSK, Schwarzburger NI, Cambaz MA, et al. Performance study of magnesium‐sulfur battery using a graphene based sulfur composite cathode electrode and a non-nucleophilic Mg electrolyte. Nanoscale. 2016;8(6):3296-3306.
100. Yu X, Manthiram A. Performance enhancement and mechanistic studies of magnesium‐sulfur cells with an advanced cathode structure. ACS Energy Letters. 2016;1(2):431-437.
101. Regulacio MD, Nguyen DT, Horia R, Seh ZW. Designing nanostructured metal chalcogenides as cathode materials for rechargeable magnesium batteries. Small. 2021;17(25):2007683.
102. Shen J, Zhang Y, Chen D, Li X, Chen Z, Cao S-a, et al. A hollow CuS nanocube cathode for rechargeable Mg batteries: effect of the structure on the performance. Journal of Materials Chemistry A. 2019;7(37):21410-21420.
103. Kravchyk KV, Widmer R, Erni R, Dubey RJ-C, Krumeich F, Kovalenko MV, et al. Copper sulfide nanoparticles as high-performance cathode materials for Mg-ion batteries. Scientific reports. 2019;9(1):1-8.
104. Wu M, Zhang Y, Li T, Chen Z, Cao S-a, Xu F. Copper sulfide nanoparticles as high-performance cathode materials for magnesium secondary batteries. Nanoscale. 2018;10(26):12526-12534.
105. Wang Z, Rafai S, Qiao C, Jia J, Zhu Y, Ma X, et al. Microwave-assisted synthesis of CuS hierarchical nanosheets as the cathode material for high-capacity rechargeable magnesium batteries. ACS applied materials & interfaces. 2019;11(7):7046-7054.
106. Shen Y, Wang Y, Miao Y, Yang M, Zhao X, Shen X. High‐Energy Interlayer‐Expanded Copper Sulfide Cathode Material in Non‐Corrosive Electrolyte for Rechargeable Magnesium Batteries. Advanced Materials. 2020;32(4):1905524.
107. Duffort V, Sun X, Nazar LF. Screening for positive electrodes for magnesium batteries: a protocol for studies at elevated temperatures. Chemical communications. 2016;52(84):12458-12461.

108. Yang X, Du C, Zhu Y, Peng H, Liu B, Cao Y, et al. Constructing defect-rich unconventional phase $Cu_{7.2}S_4$ nanotubes via microwave-induced selective etching for ultra-stable rechargeable magnesium batteries. Chemical Engineering Journal. 2022;430:133108.
109. Cao Y, Zhu Y, Du C, Yang X, Xia T, Ma X, et al. Anionic Te-Substitution Boosting the Reversible Redox in CuS Nanosheet Cathodes for Magnesium Storage. ACS nano. 2022;16(1):1578-1588.
110. He D, Wu D, Gao J, Wu X, Zeng X, Ding W. Flower-like CoS with nanostructures as a new cathode-active material for rechargeable magnesium batteries. Journal of Power Sources. 2015;294:643-649.
111. Arsentev M, Missyul A, Petrov AV, Hammouri M. TiS3 magnesium battery material: atomic-scale study of maximum capacity and structural behavior. The Journal of Physical Chemistry C. 2017;121(29):15509-15515.
112. Du A, Zhao Y, Zhang Z, Dong S, Cui Z, Tang K, et al. Selenium sulfide cathode with copper foam interlayer for promising magnesium electrochemistry. Energy Storage Materials. 2020;26:23-31.
113. Liang K, Marcus K, Guo L, Li Z, Zhou L, Li Y, et al. A freestanding NiS_x porous film as a binder-free electrode for Mg-ion batteries. Chemical Communications. 2017;53(54):7608-7611.
114. Yagi S, Ichitsubo T, Tanaka A, editors. Magnesium battery current collectors for evaluation of positive electrode active materials in a Grignard reagent-based electrolyte. ECS meeting abstracts, San Francisco, California; 2013;27.
115. Aurbach D, Suresh GS, Levi E, Mitelman A, Mizrahi O, Chusid O, et al. Progress in rechargeable magnesium battery technology. Advanced Materials. 2007;19(23):4260-4267.
116. Lee B, Cho J-H, Seo HR, Na SB, Kim JH, Cho BW, et al. Strategic combination of Grignard reagents and allyl-functionalized ionic liquids as an advanced electrolyte for rechargeable magnesium batteries. Journal of Materials Chemistry A. 2018;6(7):3126-3133.
117. Gao T, Noked M, Pearse AJ, Gillette E, Fan X, Zhu Y, et al. Enhancing the reversibility of Mg/S battery chemistry through Li^+ mediation. Journal of the American Chemical Society. 2015;137(38):12388-12393.
118. Gregory TD, Hoffman RJ, Winterton RC. Nonaqueous electrochemistry of magnesium: applications to energy storage. Journal of the Electrochemical Society. 1990;137(3):775.
119. Guo Y-s, Zhang F, Yang J, Wang F-f, NuLi Y, Hirano S-i. Boron-based electrolyte solutions with wide electrochemical windows for rechargeable magnesium batteries. Energy & Environmental Science. 2012;5(10):9100-9106.
120. Mohtadi R, Matsui M, Arthur TS, Hwang SJ. Magnesium borohydride: from hydrogen storage to magnesium battery. Angewandte Chemie. 2012;124(39):9918-9921.
121. Xu H, Zhang Z, Cui Z, Du A, Lu C, Dong S, et al. Strong anion receptor-assisted boron-based Mg electrolyte with wide electrochemical window and non-nucleophilic characteristic. Electrochemistry Communications. 2017;83:72-76.
122. Ha JH, Lee B, Lee M, Yim T, Oh SH. Al-compatible boron-based electrolytes for rechargeable magnesium batteries. Chemical Communications. 2020;56(91):14163-14166.
123. Zhu J, Guo Y, Yang J, Nuli Y, Zhang F, Wang J, et al. Halogen-free boron based electrolyte solution for rechargeable magnesium batteries. Journal of Power Sources. 2014;248:690-694.
124. Dlugatch B, Mohankumar M, Attias R, Krishna BM, Elias Y, Gofer Y, et al. Evaluation of Mg $[B(HFIP)_4]_2$-Based Electrolyte Solutions for Rechargeable Mg Batteries. ACS Applied Materials & Interfaces. 2021;13(46):54894-54905.
125. Tutusaus O, Mohtadi R, Arthur TS, Mizuno F, Nelson EG, Sevryugina YV. An efficient halogen ‐ free electrolyte for use in rechargeable magnesium batteries. Angewandte Chemie. 2015;127(27):8011-8015.

126. McArthur SG, Jay R, Geng L, Guo J, Lavallo V. Below the 12-vertex: 10-vertex carborane anions as non-corrosive, halide free, electrolytes for rechargeable Mg batteries. Chemical Communications. 2017;53(32):4453-4456.
127. Hahn NT, Seguin TJ, Lau K-C, Liao C, Ingram BJ, Persson KA, et al. Enhanced stability of the carba-closo-dodecaborate anion for high-voltage battery electrolytes through rational design. Journal of the American Chemical Society. 2018;140(35):11076-11084.
128. Sun J, Zou Y, Gao S, Shao L, Chen C. Robust Strategy of Quasi-Solid-State Electrolytes to Boost the Stability and Compatibility of Mg Ion Batteries. ACS Applied Materials & Interfaces. 2020;12(49):54711-54719.
129. Shao Y, Rajput NN, Hu J, Hu M, Liu T, Wei Z, et al. Nanocomposite polymer electrolyte for rechargeable magnesium batteries. Nano Energy. 2015;12:750-759.

List of Tables

Table 1 A comparison of different characteristics of Mg versus Li, Na, Ca, Al and Zn[12-17]

Category	Li	Mg	Na	Ca	Al	Zn
Cationic radius (Å)	0.76	0.72	1.02	1	0.53	0.74
Potential (V vs SHE)	-3.04	-2.37	-2.71	-2.87	-1.66	-0.8
Valence change	1	2	1	2	3	2
Specific Capacity (mA h g^{-1})	3861 (Li^{+})	2205 (Mg^{2+})	1161 (Na^{+})	1337 (Ca^{2+})	2980 (Al^{3+})	820 (Zn^{2+})
Volumetric Capacity (mA h cm^{-3})	2046	3832	1129	2073	8046	5854

Table 2 Summary of alloy based materials and their electrochemical performance as anodes for RMBs

Anode	**Electrolyte**	**Specific capacity (mA h g^{-1})/Current density (mA g^{-1})**	**Capacity retention (mA h g^{-1})/Cycles/Current density (mA g^{-1})**	**Rate capability (mA h g^{-1})/Current density (mA g^{-1})**	**Ref**
Bi	0.25 M EtMgCl-(Et2AlCl)2/THF	371/0.2 C		300/1 C	31
NT - Bi	0.1 M /1.5 M Mg $(BH_4)_2$ /LiBH4 in diglyme	350/0.05 C	303/200/–	216/5 C	32
NW - Bi	0.25 M Mg (AlCl2BuEt2)2 /THF	353/19.25	207/100/192.5	–/–	33
NP - Mg_3Bi_2	LiCl −APC	360/100	209/300/380	251/1900	34
$Bi_{0.6}RGO_{0.4}$	2M EtMgCl/THF	413/39	372/50/39	238/700	35
Sn	(EtMgCl, $Et_{2A}lCl$)/THF	903/0.002 C	200/10/0.01 C	200/0.05 C	36
Sn	0.5 M PhMgCl/THF	321/52	289/30/52	–/–	37
Mg_2Sn	0.5M PhMgCl/THF	270/16	197/50/16	–/–	27
Mg_2Sn /graphite	0.5 M PhMgCl/THF	382/32	270/60/32	382/32	38
$Bi_{0.55}Sb_{0.45}$	(EtMgCl, Et_2AlCl)/THF	298/–	151/100/1 C	–/–	39
SnSb	APC	420/50	260/200/50	–/–	40
P – Bi_3Sn_2	0.4 M APC	416/100	305/200/1000	367/1000	41

Eutectic Bi-Sn	0.4 M APC	538/50	233/200/–	417/1000	30
F – $Sn_{82}Bi_{18}$	0.4 M APC	600/20	40/25/20	120/1000	42
In	0.35 M (EtMgCl, Et2AlCl)/THF	425/0.02C	425/10/0.02 C	280/0.1 C	43
InBi	0.35 M (EtMgCl, Et2AlCl)/THF	410/0.01 C	280/100/0.05 C	150/1 C	44
Mg_2Ga_5	0.4 M APC + 0.4 M LiCl	306/615	212.7/1000/ 922.5	270/615	45
InSb	0.35 M (EtMgCl, Et2AlCl)/THF	535/0.2 C	350/40/0.2 C	200/0.4 C	46

Table 3 Summary of electrochemical behavior of various intercalation type cathodes for RMBs

Cathode type	**Material**	**Electrolyte**	**Discharge capacity [mA h g^{-1}]**	**Cycles/capacity [mA h g^{-1}]/ rate [mA g^{-1}]**	**Rate capacity [mA h g^{-1}]/ rate [mA g^{-1}]**	**Ref**
Chevrel phase (CP)	Mo_6S_8	0.4 M 2(PhMgCl)-$AlCl_3$ in tetrahydrofuran	76	–/–/–	66/192	49
	$CuxMo_6S_8$ (Cu-CP)	0.4 M $(PhMgCl)_2$-$AlCl_3$/tetrahydrofuran (THF)	122.9	–/–/–	123.3/5	93
2D layered materials	V_2O_5 nanowires	1 M Mg $(ClO_4)_2$/AN	103	100/36/20	130/14.73	55
	V_2O_5/carbon composite	1 M Mg $(ClO_4)_2$/AN	–	–/–/–	–/–	56
	$V_2O_5{\cdot}nH_2O$@rGO	0.5 M $Mg(TFSI)_2$ in AN	~320	200/~97/1000	~100/2000	57
	V_2O_5/PANI	APC/1.0 M LiCl	–	500/103/500	361/20	58
	Ti-V_2O_{5-x}	0.5 M $Mg(ClO_4)_2$/AN	241.3	400/195.4/–	148/500	59
	α-MoO_3 thin film	0.1 m $Mg(TFSI)_2$ in AN	220	10/210/–	–/–	60
	$Mo_{2.5+y}VO_{9+\delta}$	$Mg(TFSI)_2$	397	15/235/2	114/4	61
	MoS_2	$[Mg_2Cl_3]^+{\cdot}[AlPh_2Cl_2]^-$/THF (APC)	152	–/–/–	49/200	62
	N-CNFs@MoS_2	LiCl-APC	290	120/131/200	110/1000	63
	Graphene-like MoS_2	$Mg(AlCl_3\ Bu)_2$ in THF	170	50/~161.5/20	–/–	64
	Graphene like MoS_2/graphene	0.4 M $(PhMgCl)_2{}^-AlCl_3$/THF	115.9	50/82.5/–	–/–	65
	MoS_2@C@PANI	0.4 M $(PhMgCl)_2{}^-AlCl_3$/THF	–	100/114/100	–/–	66
	MoS_2/Ti_3C_2 MXene	0.4 M APC	165	50/108/50	93/200	68
	BC/Ti_3C_2	0.4 M $(PhMgCl)_2{}^-AlCl_3$/THF (APC)	171	100/150/50	–/–	67

	$Ti_3C_2T_x$@C nanospheres	0.4 M $Mg_2Cl_3^+ \cdot AlPh_2Cl_2^-$/THF	198.7	400/140.6/50	123.3/200	69
Prussian blue analogs (PBA)	$Na_{0.6}9Fe_2(CN)_6$	0.3 M $Mg(TFSI)_2$ in AN	70	–/–/–	–/–	72
	KNF-086	0.5 M $Mg(ClO_4)_2$ in acetonitrile	48.3	30/33/11.4	11.5/228	75
	$NaV_2O_2(PO_4)_2F$/rGO	0.3 M $Mg(TFSI)_2$ in AN	92.4	–/–/–	83.6/500	76
Polyanion compounds	$Mg_{1.03}Mn_{0.97}SiO_4$	0.25M $Mg(AlCl_2EtBu)_2$/THF	92.9	–/–/–	36.8	78
	$MgCoSiO_4$	0.25 M $Mg(AlCl_2EtBu)_2$/THF	167	–/–/–	–/–	80
	$MgFeSiO_4$	$Mg(TFSI)_2$	300	–/–/–	–/–	81
Other intercalation cathodes	$VOPO_4$	All phenyl complex (APC)	310	500/192/100	109/2000	85
	$VOPO_4$	0.1 M $Mg(ClO_4)_2.6H_2O$ in propylene carbonate (PC)	91.7	–/–/–	–/–	86
	VS_4 Nanodendrites	0.4 M 2PhMgCl-$AlCl_3$ (APC)	251	800/74/500	106/500	87
	VS_4@Ti_3C_2/C	0.25 M 2PhMgCl-$AlCl_3$/THF	492	900/147/500	129/1000	88
	TiO_2-UN@C	All phenyl complex (APC)	–	1000/61/500	–/–	84

Table 4 Summary of conversion type cathodes and their electrochemical characteristics as cathodes for RMBs

Conversion cathodes	**Cathode**	**Anode**	**Cell configuration**	**Capacity (mA h g^{-1})**	**Ref**
Redox-active organic compounds	DMBQ	Mg	Two electrode	100 mA h g^{-1}	94
	14PAQ	Mg	Two electrode	132.7 mA h g^{-1}	95
	EV	Mg	Three electrode	109.1 mA h g^{-1}	96
Sulfide materials	Graphene-Sulfur	Mg-carbon	Two electrode	448 mA h g^{-1}	99
	Sulfur coated with CNF	Mg	Two electrode	1200 mA h g^{-1}	100
	CuS nanocubes	Mg	Two electrode	200 mA h g^{-1}	102
	CuS nanosheets	Mg	Two electrode	300 mA h g^{-1}	105
	Cu7.2S4 nanotubes	Mg	Two electrode	314 mA h g^{-1}	108
	CuS1–*x*Te*x* nanosheet	Mg	Two electrode	446 mA h g^{-1}	109
	CoS nanoflowers	Mg	Two electrode	150 mA h g^{-1}	110
	NiSx porous film	Mg	Two electrode	150 mA h cm^{-3}	113

List of figures

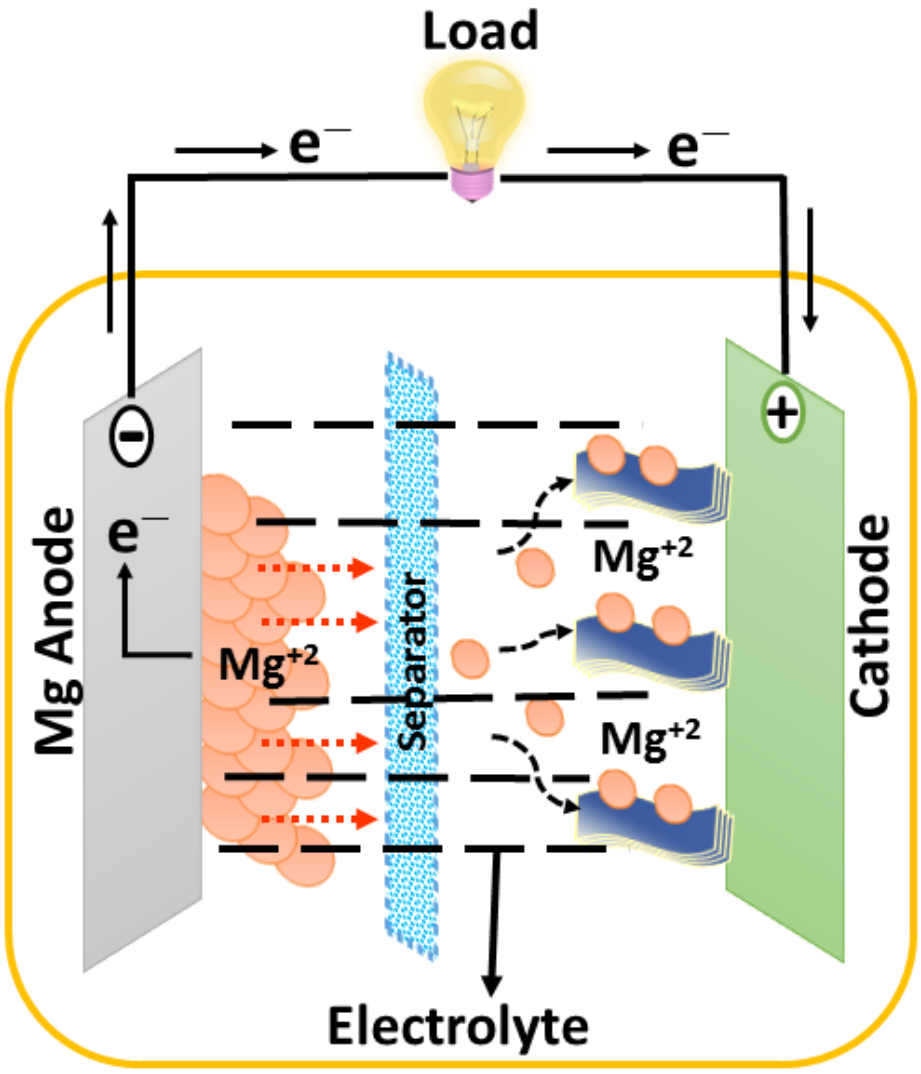

Figure 1 Schematic and working principle of typical RMB

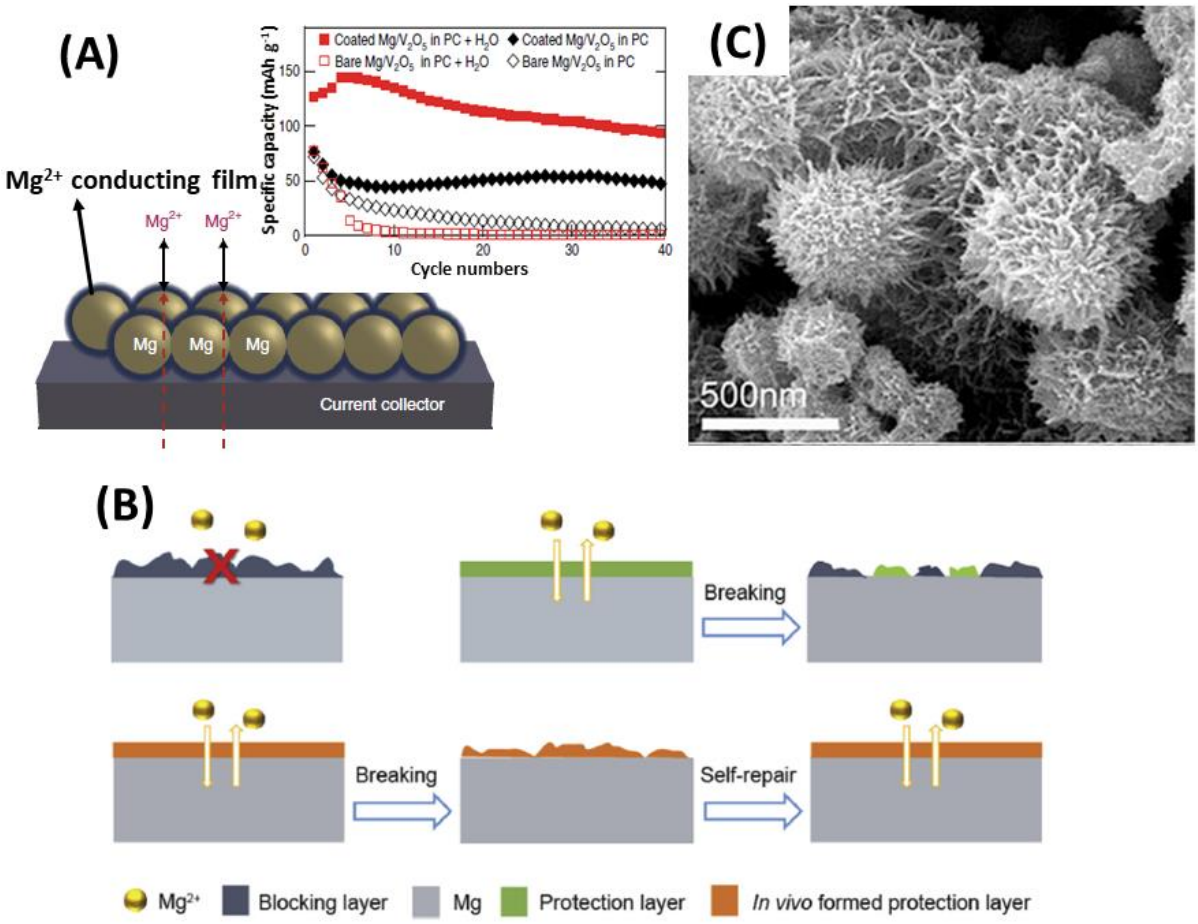

Figure 2 (A) Schematic of a Mg powder electrode coated with the artificial Mg^{2+} conducting interphase and its cyclic stability graph in nonaqueous carbonate and water-containing electrolyte[20] (B) Schematic showing the formation of Ge protection layer on Mg metal anode. Adapted with permission.[21] Copyright 2020, Elsevier, (C) SEM image of sea-urchin type nanoporous Mg[23]

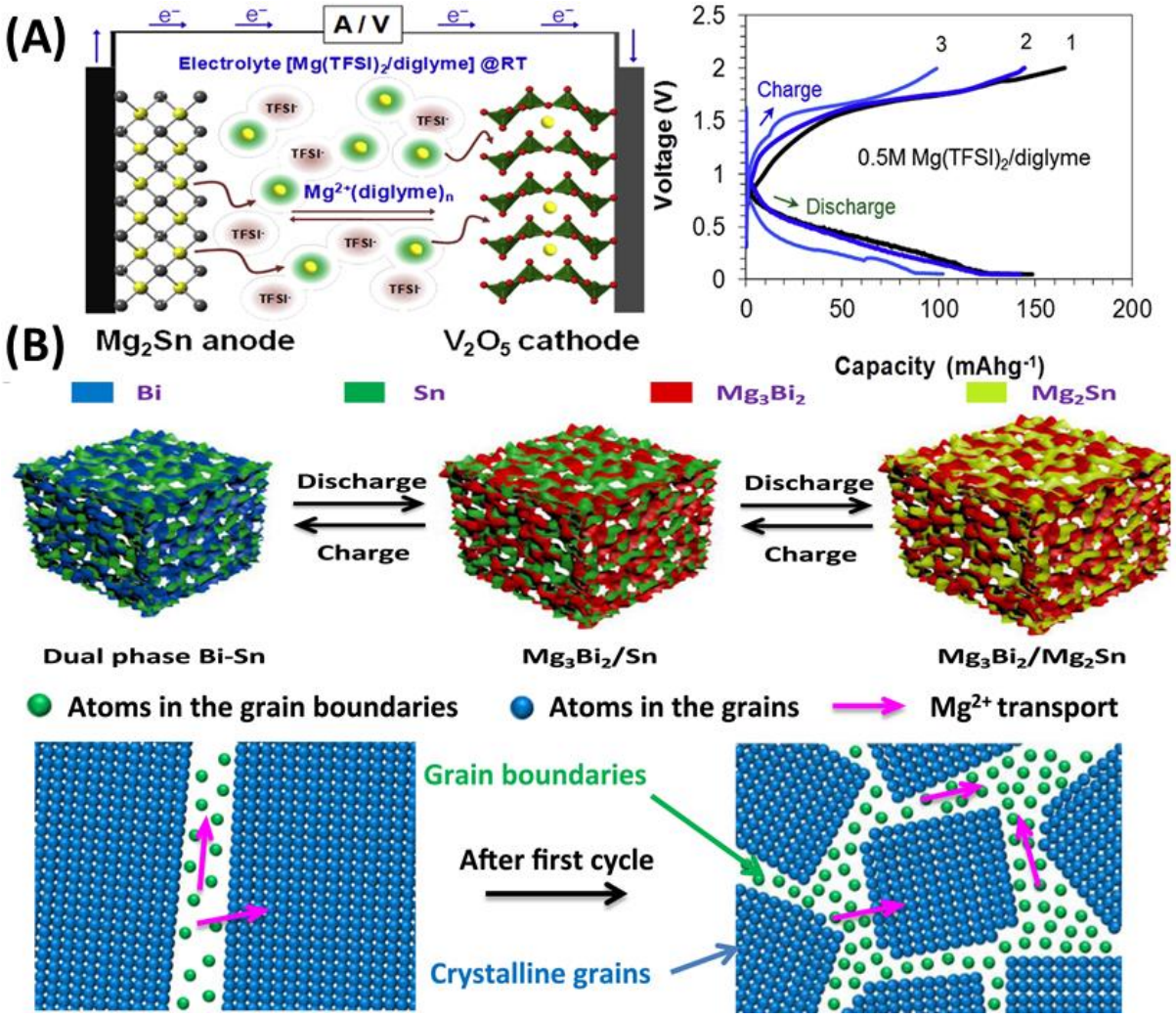

Figure 3 (A) Schematic of a battery reaction of $Mg_2Sn//V_2O_5$ Mg-ion full-cell and Voltage profile of the full cell with 0.5 M $Mg(TFSI)_2$/diglyme electrolyte at C/20. Adapted with permission.[27] Copyright 2017, Elsevier, (B) Schematic illustration of the electrochemical reaction mechanisms of nanoporous NP-Bi-Sn alloy and also the increased grain boundaries on the atomic scale after the first cycle and the enhanced Mg^{2+} transport. Adapted with permission.[29] Copyright 2017, Elsevier.

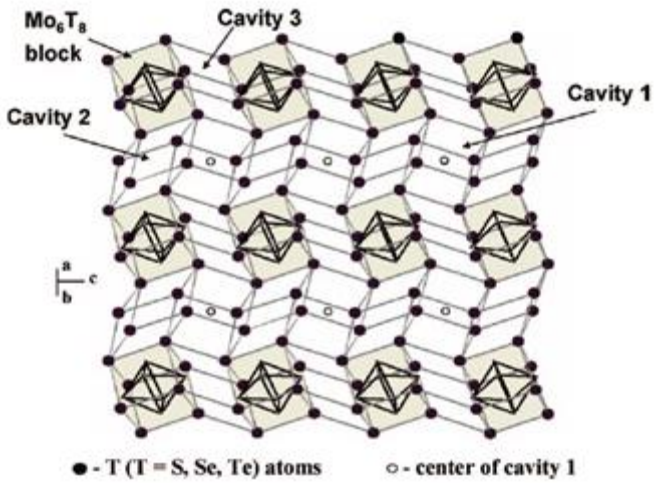

Figure 4 Basic crystal structure of Mo_6T_8 CP. Adapted with permission.[48] Copyright 2009 ACS

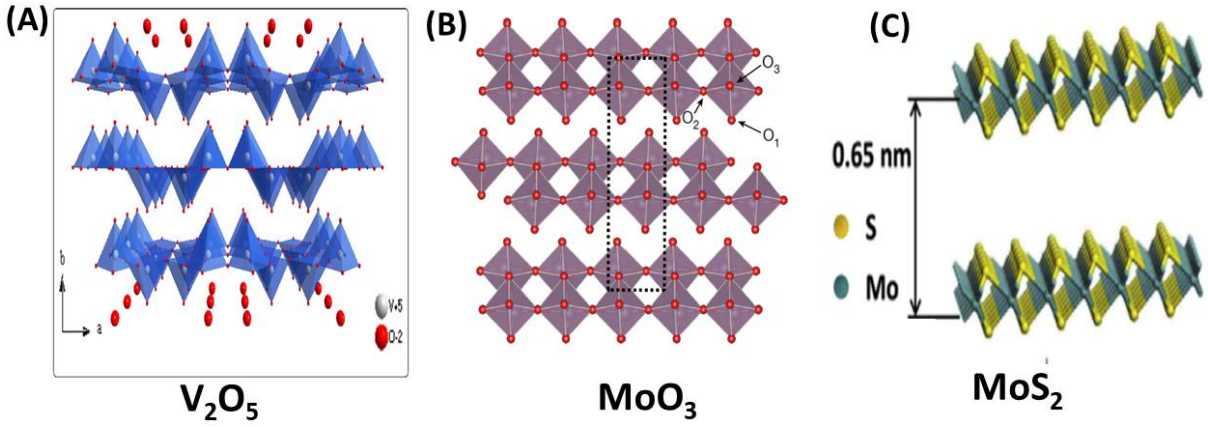

Figure 5 Crystal structure of different layered materials (A) V_2O_5[51] (B) MoO_3[52] (C) MoS_2 Adapted with permission. [53] Copyright 2015 Elsevier.

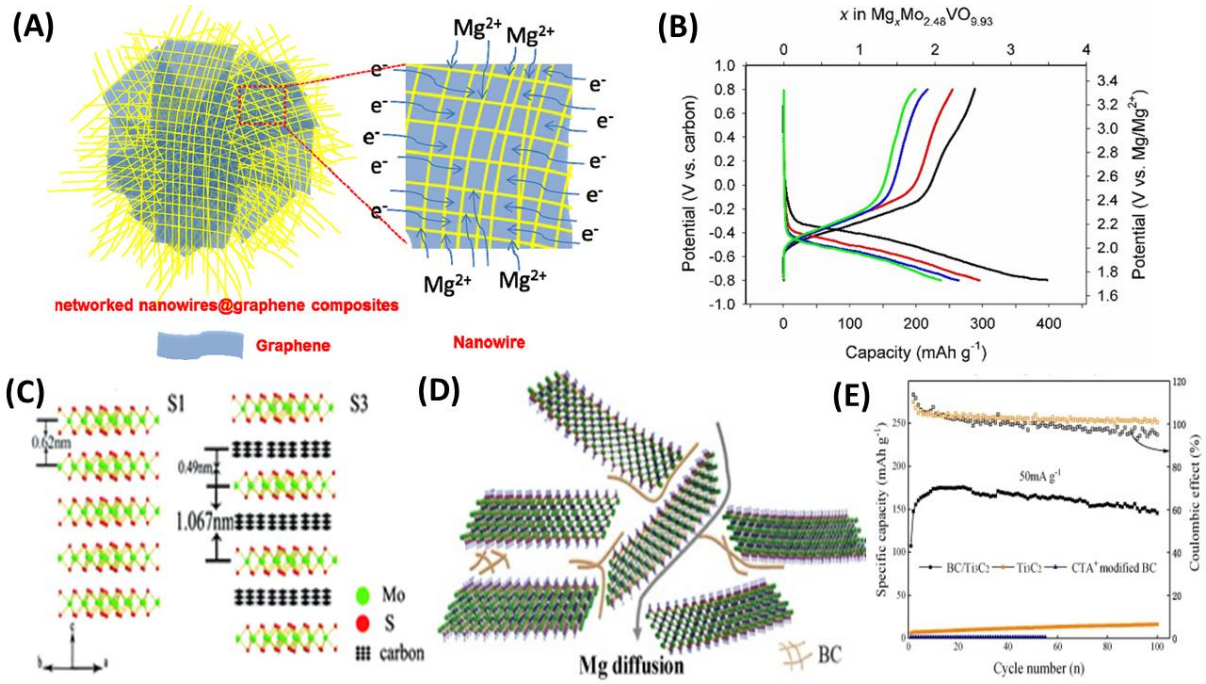

Figure 6 (A) Schematic showing the $V_2O_5.nH_2O$@rGO nanocomposite with bi-continuous electron/ion transport pathways, large area electrode/electrolyte interface, and facile strain relaxation during Mg^{2+} insertion/extraction Adapted with permission.[57] Copyright 2015 Elsevier (B) Electrochemical discharge/charge profile of AC/ $Mo_{2.48}VO_{9.93}$ cell at a rate of C/70 (2 mA g^{-1}): 1st cycle, black; 2nd cycle, red; 5th cycle, blue; 10th cycle, green Adapted with permission. [61] Copyright 2016 ACS (C) schematic illustration of microstructures of MoS_2/C[64] (D, E) Schematic illustration of Mg diffusion path in BC/Ti_3C_2 film and Cycle performance of Ti_3C_2 film, BC/Ti_3C_2 film and CTA^+ modified BC film at a current rate of 50 mA g^{-1} Adapted with permission. [67] Copyright 2020 Elsevier.

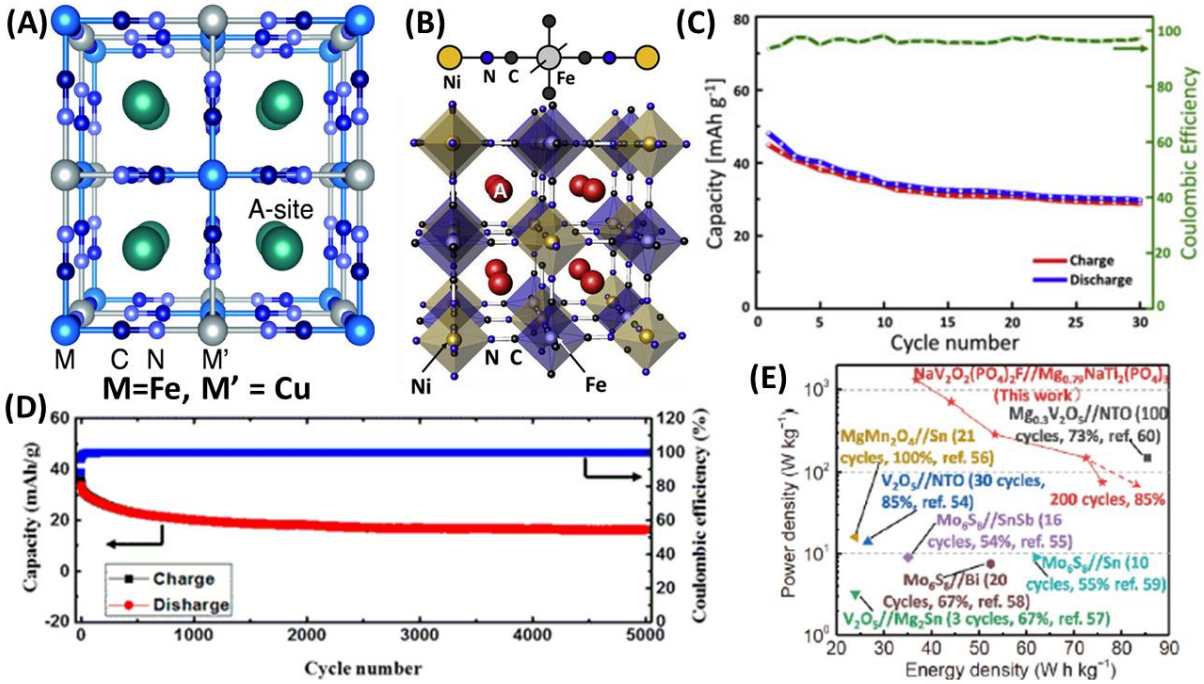

Figure 7 (A)Structure of a PBA $A_xM_y[M'(CN)_6]\cdot nH_2O$. Cations A and water are accommodated in A-sites. For CuFe-PBA, M and M' are Fe and Cu ions, respectively[73] (B, C) The unit cell structure of an ideal Prussian-blue analogue (A = metal ions, zeolitic water) and Cycle performances of the AC/KNF-086 cell at 0.2 C-rate in 0.5 M $Mg(ClO_4)_2$ in AN electrolyte. Adapted with permission [75] Copyright 2017 Elsevier (D) Cyclic, Coulombic performance of the aqueous Mg-ion battery at the current of 2 A g^{-1} between 0 and 1.55 V. Adapted with permission [74] Copyright 2017 ACS (E) Ragone plot of Mg-ion full cell with $NaV_2O_2(PO_4)_2F$/rGO cathode in organic electrolyte[76]

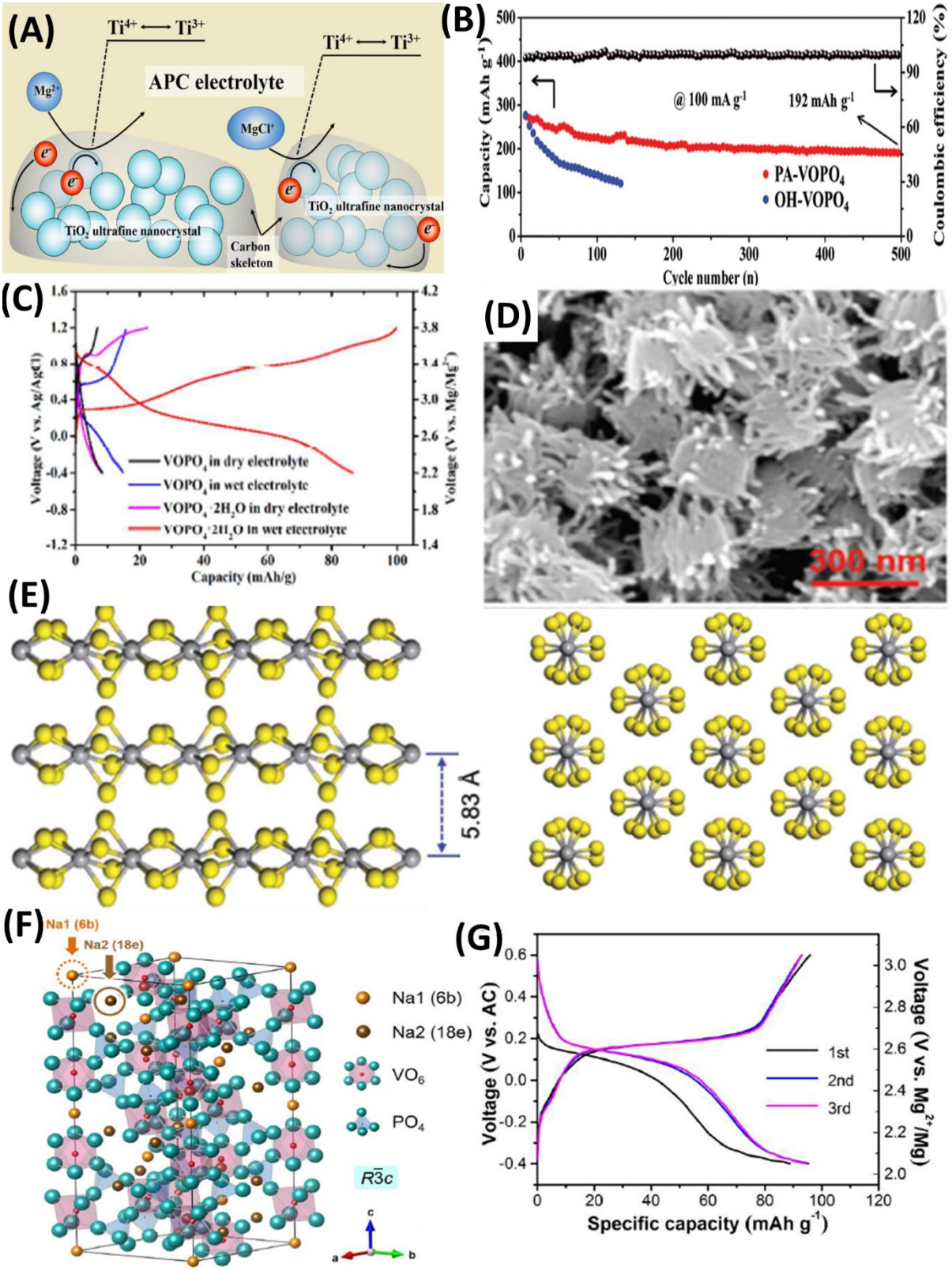

Figure 8 (A) Schematic showing the charge storage mechanism of TiO_2-UN@C in Mg metal batteries. Adapted with permission. [84] Copyright 2021 Elsevier (B) Specific capacity and Coulombic efficiency of PA-$VOPO_4$ nanosheets at 100 mA g^{-1} current density[85] (C) Voltage profiles of $VOPO_4$ and $VOPO_4$•$2H_2O$ in dry [0.1 M $Mg(ClO_4)_2$-PC] and wet [0.1 M $Mg(ClO_4)_2$•$6H_2O$-PC] electrolyte at 5 mA g^{-1} current density Adapted with permission. [86] Copyright 2018 ACS (D) SEM image of sea-urchin like VS_4 nanodendrites (E) Schematic geometries of linear-chain like VS_4 nanodendrites, showing an interval of 5.83 Å between the atomic chains[87] (F) Crystal structure of NASICON-type $Na_3V_2(PO_4)_3$ with $R\bar{3}c$

symmetry Adapted with permission. [92] Copyright 2020 ACS (G) Galvanostatic charge-discharge voltage profile of ED-NVP/C sphere at 20 mA g^{-1} current density[89]

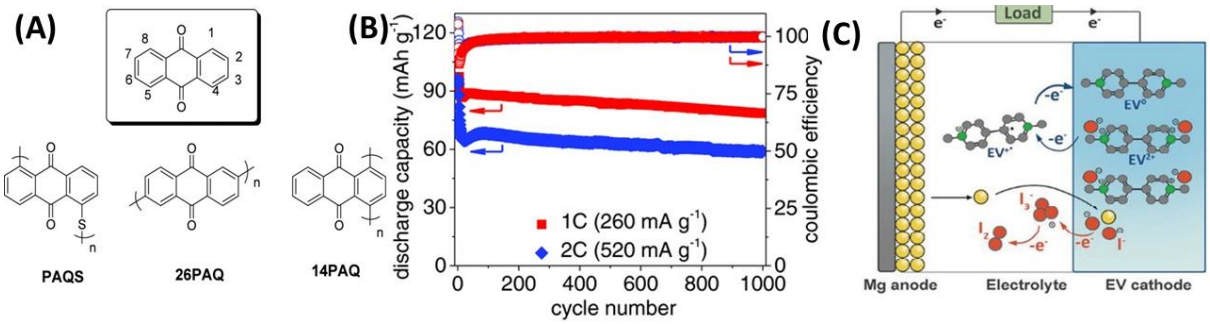

Figure 9 (A) The nomenclature of anthraquinone and the chemical structures of PAQS, 26PAQ, and 14PAQ (B) Mg-14PAQ cycling performance 1000 cycles discharge capacity and Coulombic for current rates at 1 C (260 mA g^{-1}) and 2 C (520 mA g^{-1})[95] (C) Schematic illustration of Mg/EV battery[96]

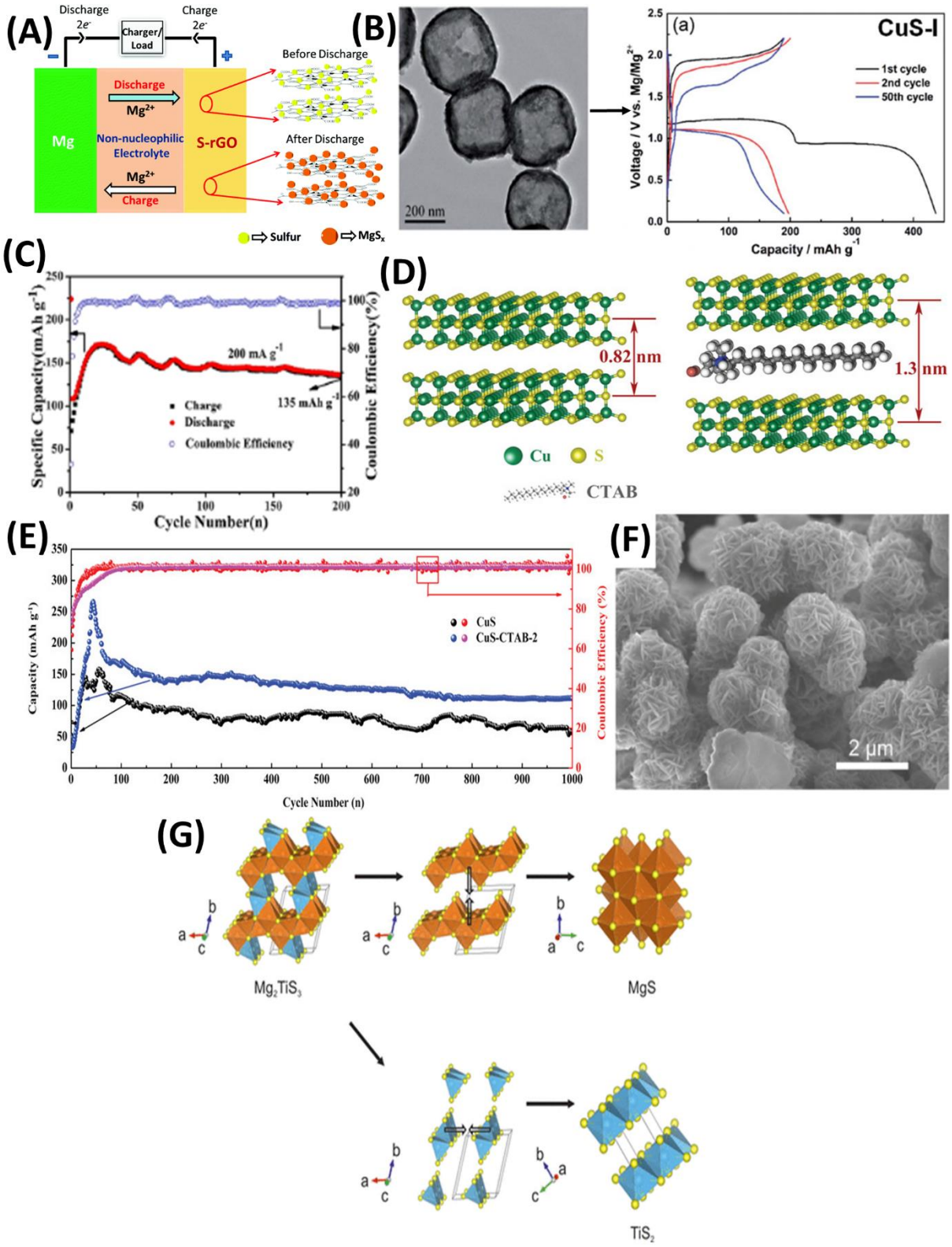

Figure 10 (A) Electrochemical mechanism of the S–rGO nanocomposite electrode within a Mg-S cell[99] (B) TEM image of CUS-1 nanocubes along with its discharge/charge profile at 100 mA g^{-1} current density[102] (C) Discharge−charge curves for CuS at different cycles at 100 mA g^{-1} current density Adapted with permission. [105] Copyright 2019 ACS (D, E) structural schematic of CuS and CuS-CTAB-2 materials and Galvanostatic charge and discharge profiles of the CuS-CTAB-2 cathode at different current densities [106] (F) SEM image of CoS nanoflower Adapted with permission. [110] Copyright 2015

Elsevier (G) Possible mechanism of the structural decomposition of the Mg-intercalated TiS_3 into MgS and TiS_2 Adapted with permission [111] Copyright 2017 ACS